

Quantum mechanics at the nanoscale

HANDE TOFFOLI

July 2, 2018

Contents

1 Preliminaries	1
1.1 Particle in a box — infinite barrier	1
1.2 Particle in a box — finite barrier	3
1.3 The variational principle	4
1.3.1 The approximate wavefunction	4
1.3.2 Variation with respect to coefficients (linear variation) and Lagrange multipliers	6
1.4 Fermi's Golden Rule	7
2 Fundamentals of Solid State Theory	11
2.1 What defines a crystal?	11
2.2 Reciprocal space	13
2.2.1 An example : Face-centered cubic lattice and its Brillouin zone	16
2.2.2 The Brillouin Zone	16
2.2.3 Bloch's theorem	18
2.3 Band structure	19
2.3.1 The Krönig-Penney model	19
2.3.2 The tight-binding approximation	22
3 The concept of confinement	25
3.1 Density of free-particle states in three, two and one dimensions	25
3.2 2-dimensional confinement — 2-dimensional electron gas	27
3.3 1-dimensional confinement — Nanowires	29
3.4 0-dimensional confinement — Quantum dots	30
3.5 A different manifestation of confinement — graphene and nanotubes	30
4 Optical properties of confined structures	35

1

Preliminaries

1.1 Particle in a box — infinite barrier

The simplest quantum mechanical system is the free-particle whose Hamiltonian simply consists of the kinetic energy term without any potential energy term

$$\hat{H} = -\frac{\hbar^2}{2m}\nabla^2. \quad (1.1)$$

The Schrödinger equation

$$\hat{H}\Psi(\vec{r}) = -\frac{\hbar^2}{2m}\nabla^2\Psi(\vec{r}) = E\Psi(\vec{r}) \quad (1.2)$$

yields the solutions

$$\Psi_{\vec{k}} = Ce^{i\vec{k}\cdot\vec{r}} \quad (1.3)$$

where C is a normalization constant. These solutions are referred to as *planewaves* since they resemble propagating fronts of simple particle waves and their energy spectrum is continuous.

When, on the other hand, the system is subject to a potential in the form of finite or infinite potential barriers, surrounding a region with zero potential, the system becomes *confined*, in other words the wavefunction becomes localized in a region in space.

In order to understand confinement, let us start with a simple problem, the *one-dimensional particle in a box*, which is described by a zero potential region between two infinitely tall barriers

$$V(x) = \begin{cases} 0 & \text{if } 0 < x < L \\ \infty & \text{otherwise} \end{cases} \quad (1.4)$$

The barriers at $x = 0$ and $x = L$ are impenetrable even for quantum mechanical systems. Hence, the wavefunctions $\psi(x)$ to the left and the right of the *quantum well* (another name for box) are all zero. Inside the well, the Schrödinger equation is the same as that of a free particle, given in Eq. 1.2. We are then looking for solutions, $\psi(x)$, which return themselves times a constant when differentiated twice. The family of general solutions to this kind of differential equations are: $\sin(kx)$, $\cos(kx)$, $e^{\kappa x}$ and $e^{-\kappa x}$. Of these solutions, we immediately eliminate the exponential functions as they correspond to exponential decay or growth at the boundaries. $\cos(kx)$ is also eliminated since it has a value of 1 at $x = 0$, which violates the continuity of the solution. By this process of elimination, we then expect the solutions to be purely sinusoidal. Furthermore, the wavelengths of the solutions must fit exactly within the boundaries of the box and thus cannot take any arbitrary value. With these constraints, the wavefunctions and the

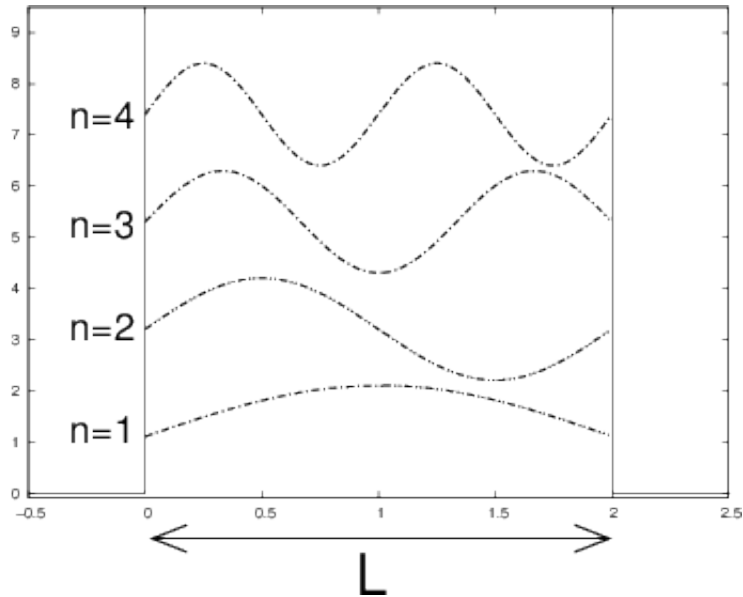


Figure 1.1: Solutions of the infinite potential well.

corresponding eigenenergies are (see Fig. 1.1)

$$\psi_n(x) = \sqrt{\frac{2}{L}} \sin(k_n x) \quad (1.5)$$

$$E_n = \frac{k_n^2 \hbar^2}{2m} \quad (1.6)$$

where L is the width of the one-dimensional box and k_n is the wavevector given by

$$k_n = \frac{\pi n}{L} \quad n = 0, 1, 2, \dots \quad (1.7)$$

The prefactor, $\sqrt{2/L}$, in the solutions is the normalization constant. A few eigenfunctions corresponding to the lowest-lying states have been demonstrated in Fig. 1.1. The functions have been displaced vertically to guide the eye.

Let us now generalize the particle in a box problem to three dimensions, which corresponds to a cubic box. For simplicity we shall assume that the edges of the box in each dimension are the same. The states are then going to be given by

$$\psi_{n_x n_y n_z}(\vec{r}) = \left(\frac{2}{L}\right)^{3/2} \sin(k_{n_x} x) \sin(k_{n_y} y) \sin(k_{n_z} z) \quad (1.8)$$

where the relation in Eq. 1.7 applies to all three dimensions separately. Similarly the eigenenergies are

$$E_{n_x, n_y, n_z} = \frac{k_{n_x}^2 \hbar^2}{2m} + \frac{k_{n_y}^2 \hbar^2}{2m} + \frac{k_{n_z}^2 \hbar^2}{2m} \quad (1.9)$$

The important point to notice here is that in both systems above, as the size of the system decreases the distance between energy levels decrease. Thus in order for the eigenenergies of the system to be distinguished by the resolution of the devices in experiments, the system size must be sufficiently small. No system can be exactly modeled by a particle in a box, however today's technology is able to produce materials that at least partially display some characteristics.

1.2 Particle in a box — finite barrier

Realistically speaking, no confinement is perfect. In other words, the potential barrier at the surface or interface of nanostructures is finite. In that case, the amplitude of the wavefunction outside of the box is not zero. The potential for this kind of a finite barrier can be written as

$$V(x) = \begin{cases} V_0 & \text{if } |x| < L/2 \\ 0 & \text{otherwise} \end{cases} \quad (1.10)$$

In Eq. 1.10, the magnitude of the potential barrier is denoted by V_0 . Note that, for mathematical convenience, we consider a symmetric well with respect to the origin in contrast with the infinite well. The energies corresponding to the eigenvalues of the corresponding Schrödinger equation for a finite well can be classified into two: bound states ($E < V_0$) and unbound states ($E > V_0$). In this section, we will only concern ourselves with bound states. The solutions are further classified according to their parity. The even solutions are characterized by inversion symmetry with respect to the middle of the well. Within the well, the Schrödinger equation is the same as Eq. 1.2 and therefore the solutions are expected to be sinusoidal while outside, they should decay to zero as we move further away from the well. As a result, the even solutions, along the entire x -axis, have the following form:

$$\psi(x) = \begin{cases} A \cos(qx) & |x| < L/2 \\ B e^{-\beta|x|} & |x| > L/2 \end{cases} \quad (1.11)$$

where q and β are defined as

$$\begin{aligned} q &= \sqrt{\frac{2mE}{\hbar^2}} \\ \beta &= \sqrt{\frac{2m(V_0 - E)}{\hbar^2}} \end{aligned} \quad (1.12)$$

Since we are considering only bound states, β in Eq. 1.12 runs no risk of being complex. The arbitrary coefficients in Eq. 1.11, A and B can be determined with the help of boundary conditions, which require continuity. This means that both the wave function itself and its derivative must be equal at $x = \mp L/2$. The two boundaries yield identical results so we only consider $x = L/2$. Continuity at $x = L/2$ yields two equations:

$$A \cos \frac{qL}{2} = B \exp \left(-\frac{\beta L}{2} \right) \quad (1.13)$$

$$Aq \sin \frac{qL}{2} = B\beta \exp \left(-\frac{\beta L}{2} \right) \quad (1.14)$$

Dividing Eq. 1.14 by Eq. 1.13, we obtain the transcendental equation

$$\tan \frac{qL}{2} = \frac{\beta}{q}. \quad (1.15)$$

A similar argument can be made for the odd-parity solutions and yields

$$\tan \frac{qL}{2} = -\frac{q}{\beta}. \quad (1.16)$$

To unify the odd and even solutions, consider the trigonometric identity

$$\tan 2x = \frac{2 \tan x}{1 - \tan^2 x} \quad (1.17)$$

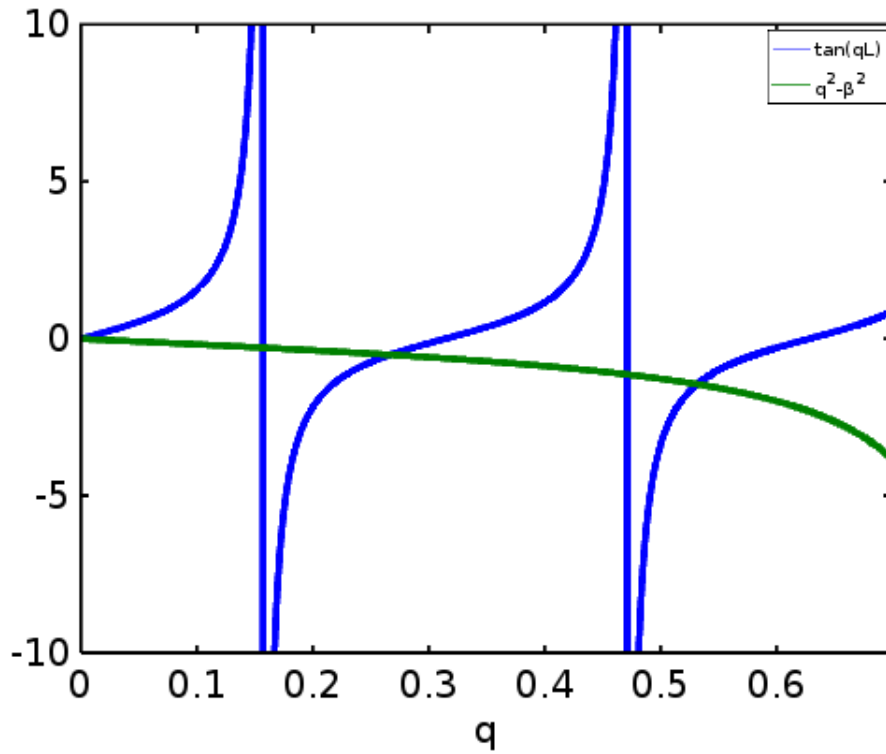


Figure 1.2: Allowed solutions of the finite barrier.

For the even solutions, Eq. 1.17 can be developed as follows:

$$\tan qL = \frac{2\frac{\beta}{q}}{1 - \frac{\beta^2}{q^2}} = \frac{2\beta q}{q^2 - \beta^2} \quad (1.18)$$

Similarly, for the odd solutions it gives

$$\tan qL = \frac{-2\frac{q}{\beta}}{1 - \frac{q^2}{\beta^2}} = \frac{2\beta q}{q^2 - \beta^2} \quad (1.19)$$

Thus, a unified compatibility equation for both parities is given by the equation,

$$\tan qL = \frac{2q\beta}{q^2 - \beta^2}. \quad (1.20)$$

This equation can be solved numerically by means of plotting the left and right hand sides of Eq. 1.20. The intersection points of the blue and green curves in Fig. 1.2 are the solutions of Eq. 1.20. The example seen in Eq. 1.2 was created for a finite barrier of height $V_0 = 5$ eV and width 10 \AA . The energies of the solutions are 0.27, 1.08, 4.06 eV.

1.3 The variational principle

1.3.1 The approximate wavefunction

In quantum mechanics, the main task is to solve the Schrödinger equation,

$$\hat{H}\psi = E\psi. \quad (1.21)$$

The Schrödinger equation is exactly solvable for a very narrow class of systems. In cases where the exact solution cannot be attained, the wavefunction may be approximated by a form that is easier to handle mathematically

$$\phi \approx \psi. \quad (1.22)$$

In most cases, we are interested in the ground state of the system, which we shall denote by ψ_0 yielding the ground state energy, E_0 . The excited states of the system will be denoted by $\{\psi_1, \psi_2, \dots\}$ with corresponding energies $\{E_1, E_2, \dots\}$. In what follows, we will be interested in obtaining an approximation to ψ_0

Unless we are very lucky, the approximate wavefunction ϕ will no longer be an eigenvalue of the Hamiltonian operator, \hat{H} . The quality of the approximation is assessed based on how close the expectation value of \hat{H} for ψ given by

$$\tilde{E} = \frac{\langle \phi | \hat{H} | \phi \rangle}{\langle \phi | \phi \rangle} \quad (1.23)$$

comes to the actual energy eigenvalue, E_0 . Assuming that the eigenstates of \hat{H} form a complete basis set, we may expand any other wavefunction of the system in terms of them. This observation applies also to our approximation, ϕ . We therefore write down the following expansion

$$|\phi\rangle = \sum_n c_n |\psi_n\rangle \quad (1.24)$$

where c_n are the expansion coefficients. The eigenstates $\{|\psi_n\rangle\}$ are assumed to be orthonormal. This assumption does not cause us to lose any generality because any complete set of eigenstates may be constructed to be orthonormal. Thus, the following property is satisfied

$$\langle \psi_n | \psi_m \rangle = \delta_{nm} \quad (1.25)$$

We make the further assumption that the eigenvalues, $\{E_n\}$ are labeled in an increasing order, i.e.

$$E_0 \leq E_1 \leq E_2 \leq \dots \quad (1.26)$$

Substituting Eq. 1.24 into Eq. 1.23, we obtain the following

$$\tilde{E} = \frac{\langle \phi | \hat{H} | \phi \rangle}{\langle \phi | \phi \rangle} = \frac{\sum_{nm} c_n^* c_m \langle \psi_n | \hat{H} | \psi_m \rangle}{\sum_{nm} c_n^* c_m \langle \psi_n | \psi_m \rangle} \quad (1.27)$$

$$= \frac{\sum_{nm} c_n^* c_m E_n \langle \psi_n | \psi_m \rangle}{\sum_{nm} c_n^* c_m \langle \psi_n | \psi_m \rangle} = \frac{\sum_n |c_n|^2 E_n}{\sum_n |c_n|^2} \quad (1.28)$$

The last two equalities are a result of the fact that $\{|\psi_n\rangle\}$ are eigenstates of \hat{H} and of orthonormality as stated in Eq. 1.25. If we now substitute all E_n in Eq. 1.28 with E_0 , we have

$$\tilde{E} = \frac{\sum_n |c_n|^2 E_n}{\sum_n |c_n|^2} \leq \frac{\sum_n |c_n|^2 E_0}{\sum_n |c_n|^2} = E_0 \quad (1.29)$$

where Eq. 1.26 has been utilized. We thus arrive at the central result that makes the variational method possible and practical:

Any approximation to the ground state wavefunction will yield an expectation value of the Hamiltonian that is greater than or equal to the ground state energy. Equality is satisfied only in the case that the approximate wavefunction is also a ground state wavefunction.

In practice, the approximate wavefunction is written in terms of one or more parameters,

$$\phi = \phi(p_1, p_2, \dots, p_N). \quad (1.30)$$

The set of parameters that yield the best estimate to the ground state energy within the limits of the chosen form of ϕ satisfies

$$\frac{\partial \tilde{E}(p_1, p_2, \dots, p_N)}{\partial p_1} = \frac{\partial \tilde{E}(p_1, p_2, \dots, p_N)}{\partial p_2} = \dots = \frac{\partial \tilde{E}(p_1, p_2, \dots, p_N)}{\partial p_N} = 0 \quad (1.31)$$

1.3.2 Variation with respect to coefficients (linear variation) and Lagrange multipliers

A very important class of electronic structure methods have variational origin. These methods make the initial assumption that the approximate wavefunction is a *sum* of functions satisfying intuitive properties and makes a variation over the expansion coefficients. Let us assume that the approximate wavefunction for a given system may be expanded in terms of a particular set of orbitals. Because we cannot work with an infinitely many number of such orbitals we truncate the sum and just consider the first N terms :

$$\phi(\vec{x}) = \sum_{i=1}^N c_i \chi_i(\vec{x}) \quad (1.32)$$

For each k , we would like the above expansion to satisfy the minimization condition, i.e.

$$\frac{\partial}{\partial c_k^*} \frac{\langle \phi | \hat{H} | \phi \rangle}{\langle \phi | \phi \rangle}. \quad (1.33)$$

In addition, we require the approximate wavefunction to remain normalized

$$\langle \phi | \phi \rangle = 1 \quad (1.34)$$

which then allows us to rewrite Eq. 1.33 as

$$\frac{\partial}{\partial c_k^*} \langle \phi | \hat{H} | \phi \rangle = 0 \quad (1.35)$$

We may in fact, satisfy both Eq. 1.33 and Eq. 1.34 by introducing a new quantity

$$K = \langle \phi | \hat{H} | \phi \rangle - \lambda [\langle \phi | \phi \rangle - 1] \quad (1.36)$$

and extending the minimization property to include the extra parameter λ ,

$$\frac{\partial K}{\partial c_k^*} = \frac{\partial K}{\partial \lambda} = 0 \quad (1.37)$$

Inserting Eq. 1.36 into Eq. 1.37 immediately yields

$$\langle \phi | \phi \rangle - 1 = 0 \quad (1.38)$$

and proves that minimizing K with respect to *all* of the parameters involved satisfies both of the conditions that we were aiming to satisfy. This method of introducing new variables into the problem to satisfy constraints is often used in classical and quantum mechanics. We may

introduce as many variables into the problem as there are constraints. These variables are called *Lagrange multipliers*. The Lagrange multipliers are introduced as arbitrary parameters initially, however we shall see later on that they may correspond to physically meaningful quantities.

Inserting the expansion in Eq. 1.32 into Eq. 1.35 yields

$$\begin{aligned} & \frac{\partial}{\partial c_k^*} \left[\langle \sum_i c_i \chi_i | \hat{H} | \sum_j c_j \chi_j \rangle - \lambda \left(\langle \sum_i c_i \chi_i | \sum_j c_j \chi_j \rangle - 1 \right) \right] \\ &= \frac{\partial}{\partial c_k^*} \sum_{i,j} c_i^* c_j [\langle \chi_i | \hat{H} | \chi_j \rangle - \lambda \langle \chi_i | \chi_j \rangle] \\ &= \sum_j c_j [\langle \chi_k | \hat{H} | \chi_j \rangle - \lambda \langle \chi_k | \chi_j \rangle] = 0 \end{aligned} \quad (1.39)$$

Rearranging Eq. 1.39, we obtain

$$\sum_j \langle \chi_k | \hat{H} | \chi_j \rangle c_j = \lambda \sum_j \langle \chi_k | \chi_j \rangle c_j \quad (1.40)$$

which we recognize immediately as a *generalized* eigenvalue equation

$$\mathbf{H} \cdot \mathbf{C} = \lambda \cdot \mathbf{S} \cdot \mathbf{C} \quad (1.41)$$

where \mathbf{H} and \mathbf{S} are the matrix representations of the Hamiltonian and overlap operators and their elements are defined by.

$$\begin{aligned} H_{nm} &= \langle \chi_n | \hat{H} | \chi_m \rangle \\ S_{nm} &= \langle \chi_n | \chi_m \rangle \end{aligned} \quad (1.42)$$

λ in Eq. 1.41 corresponds to a diagonal matrix whose elements on the diagonal are the eigenvalues.

If we use N basis functions to expand the trial function ϕ , Eq. 1.41 then gives N eigenvalues. But what do the eigenvalues correspond to? In order to see that let's sum both sides of Eq. 1.40 and isolate λ :

$$\lambda = \frac{\sum_{j,k} c_k^* c_j \langle \chi_k | \hat{H} | \chi_j \rangle}{\sum_{j,k} c_k^* c_j \langle \chi_k | \chi_j \rangle} = \frac{\langle \phi | \hat{H} | \phi \rangle}{\langle \phi | \phi \rangle}. \quad (1.43)$$

Eq. 1.43 implies that each of the N eigenvectors correspond to a series of expansion coefficients yielding different ϕ 's and each λ corresponds to a different expectation value. The eigenvector corresponds to the smallest eigenvalue then corresponds to the best ϕ and the smallest eigenvalue itself is the closest approximation to the ground state energy for the approximate form in Eq. 1.32.

1.4 Fermi's Golden Rule

Fermi's Golden Rule is a very popular formulation of the rate of electronic transitions between quantum mechanical states of a system. As both the characterization of nanoscale materials and their operation in applications often rely on such transitions, we give a brief review here. Fermi's Golden Rule is derived via a perturbation theory treatment of the full Hamiltonian and as such, its domain of application is only over small deviations from the exactly solvable Hamiltonian.

The starting point is a Hamiltonian that can be written as

$$H = H_0 + H'$$

where H_0 is the unperturbed part whose eigenstates are assumed to be analytically or numerically accessible and $H' = H'(t)$ is a small, possibly time-dependent perturbation. The time-dependent Schrödinger equation for H_0 is

$$i\hbar \frac{\partial \psi_0}{\partial t} = H_0 \psi_0 \quad (1.44)$$

where ψ_0 is a time-dependent state that can be written as a linear combination of time-independent, unperturbed, eigenstates $u_n^0(x, y, z)$ of H_0 as

$$\psi_0(x, y, z; t) = \sum_n a_n^0 u_n^0(x, y, z) e^{-iE_n^0 t/\hbar}. \quad (1.45)$$

where a_n are the coefficients. The time-dependent solutions of the Schrödinger equation for the full Hamiltonian are

$$H\psi = i\hbar \frac{\partial \psi}{\partial t} = (H_0 + H')\psi \quad (1.46)$$

and a similar expansion to Eq. 1.45 can be written down for ψ using the same set of unperturbed solutions $\{u_n^0(x, y, z)\}$ since presumably, they should form a complete and orthonormal set¹:

$$\psi(x, y, z; t) = \sum_n a_n(t) u_n^0 e^{-iE_n^0 t/\hbar}. \quad (1.47)$$

The only difference is that the time-dependence of the perturbing potential, H' , is reflected in the time-dependent coefficients. Substituting Eq. 1.47 into Eq. 1.46 yields

$$i\hbar \sum_n u_n^0 \frac{\partial}{\partial t} (a_n(t) e^{-iE_n^0 t/\hbar}) = \sum_n a_n(t) H |u_n^0\rangle e^{-iE_n^0 t/\hbar}. \quad (1.48)$$

Developing the left-hand-side by taking the derivative and the right-hand-side by applying the Hamiltonian yields

$$i\hbar \sum_n u_n^0 \left(\dot{a}_n(t) - i \frac{E_n^0}{\hbar} a_n(t) \right) e^{-iE_n^0 t/\hbar} = \sum_n a_n(t) (E_n^0 + H' |u_n^0\rangle) e^{-iE_n^0 t/\hbar} \quad (1.49)$$

In Eq. 1.49, we notice right away that the second term on the left and the first term on the right cancel each other out. In order to isolate an arbitrary coefficient $a_m(t)$, we multiply Eq. 1.48 from the left by $\langle u_m^0 |$ and use the orthonormality condition. This yields

$$\dot{a}_m = \frac{-i}{\hbar} \sum_n a_n(t) \underbrace{\langle u_m^0 | H' | u_n^0 \rangle}_{H'_{mn}} e^{i(E_m^0 - E_n^0)t/\hbar}. \quad (1.50)$$

Integrating both sides of Eq. 1.50 yields

$$a_m(t) - a_m(0) = \frac{-i}{\hbar} \sum_n H'_{mn} \int_0^t a_n(\tau) e^{i\omega_{mn}\tau} d\tau \simeq \frac{-i}{\hbar} \sum_n H'_{mn} \int a_n(0) (i\omega_{mn}) (e^{i\omega_{mn}t} - 1) \quad (1.51)$$

where $\hbar\omega_{mn} = E_m^0 - E_n^0$ and we have used the fact that for small perturbations $a_n(t)$ does not change very much from $a_n(0)$ so that they were interchangeable on the right-hand-side. The

¹Any complete set of nonorthonormal basis functions can be orthonormalized by means of the Gram-Schmidt scheme, so there is no loss of generality here.

probability of finding the system in state m is $|a_m(t)|^2$. Assuming that the system starts out in state n so that $a_n(0) = 1$ and all other $a_n = 0$, Eq. 1.51 yields

$$|a_m(t)|^2 = 4 (H'_{mn})^2 \sin^2 \left(\frac{\omega_{mn}t}{2} \right) / (\hbar^2 \omega_{mn}^2). \quad (1.52)$$

Note that if the final state in the transition is in the continuum, the single final state can be replaced by a density of states. But for the discrete states at hand, the transition probability to any state out of state n is

$$P(t) = \sum_m |a_m(t)|^2 = 4 |H'_{mn}|^2 \sum_m \sin^2 \left(\frac{\omega_{mn}t}{2} \right) / (\hbar^2 \omega_{mn}^2). \quad (1.53)$$

If the final states are in the continuum, the sum can be converted into an integral

$$P(t) = 4 |H'_{mn}|^2 \int_{-\infty}^{\infty} \rho(E_m) \sin^2 \frac{\omega_{mn}t/2}{\hbar^2 \omega_{mn}^2} d\hbar \omega_{mn}. \quad (1.54)$$

The largest contribution to this integral comes from $\omega_{mn} = 0$, which amounts to the approximation $\rho(E_m) \sim \rho(E_n)$. This way, $\rho(E_m)$ can be taken out of the integral and the remaining integral yields $\int \sin^2(\alpha x^2)/x^2 = \pi\alpha$. Therefore, Eq. 1.54 reduces to

$$P(t) = 4 |H'_{mn}|^2 \rho(E_n) (\pi t / 2\hbar). \quad (1.55)$$

Finally the rate of transition $R = dP/dt$ is equal to

$$R = \frac{2\pi}{\hbar} \rho(E_n) |H'_{mn}|^2. \quad (1.56)$$

2

Fundamentals of Solid State Theory

2.1 What defines a crystal?

A *crystal*, in the parlance of solid state physics, is an infinite, periodic repetition of a set of nuclei in space. Any periodic system of objects can be generated by repeatedly translating any of its legitimate subunits. Consider the simplest possible two-dimensional crystal, a square lattice. This lattice can be generated in infinitely many ways. Figure 2.1 represents a few of the possibilities: Each subunit depicted in Fig. 2.1 is referred to as a *unit cell* while the smallest possible unit cell is the so-called *primitive unit cell*. You will notice that there are three valid geometric shapes for unit cells: a square, a rectangle and a parallelepiped. The boundaries of each unit cell is delimited by two vectors (three for three-dimensional crystals), called the *lattice vectors*. The lattice vectors, the number of points per unit cell¹ and the area of each of the unit cells in Fig. 2.1 are listed in Table 2.1. Here, we assume that the distance between two neighboring points, in other words *the lattice constant*, is a . As one may expect, the larger unit cells also contain a large number of points. Any lattice that can be generated by means of two (three in 3D) noncollinear (noncoplanar in 3D) lattice vectors is called a *Bravais lattice*. While unit cell 1 (the primitive unit cell) contains one point (atom, ion, molecule) only, the other two have more. In this case, it is not enough just to replicate the unit cell but its contents must also be replicated to correctly generate the same lattice. Therefore, in addition to the lattice vectors, one also needs to specify the *basis vectors*. The basis vectors for unit cell 3, for instance, are as

¹Note that while counting the number of points contained in each unit cell, the points that correspond to the corners and sides of the unit cells contribute fractionally. For instance, each corner of unit cell 1 contributes a quarter of a point so that the unit cell has only one point. If this confuses you, you may translate the unit cell so that no corner or side goes through any points. This way, each point is entirely inside every unit cell.

Table 2.1: The lattice vectors, number of points and area in each unit cell depicted in Fig. 2.1

Unit cell	Lattice vectors	No. points	Area
1	$\vec{a}_1 = a(1, 0)$ $\vec{a}_2 = a(0, 1)$	1	a^2
2	$\vec{a}_1 = a(3, 0)$ $\vec{a}_2 = a(0, 2)$	6	$6a^2$
3	$\vec{a}_1 = a(1, 0)$ $\vec{a}_2 = a(3, 2)$	2	$2a^2$

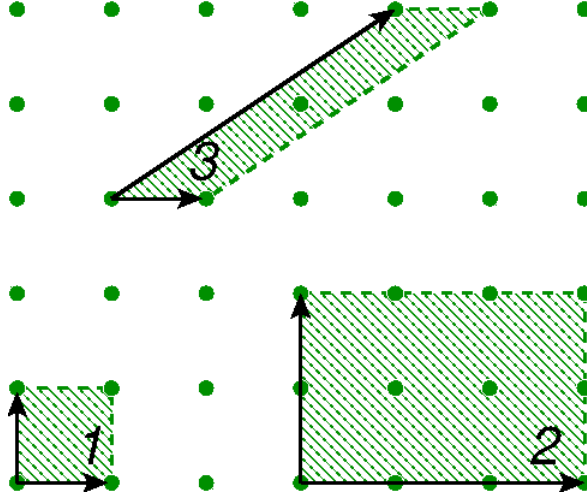


Figure 2.1: A square lattice in two dimensions and a few of the infinitely many subunits that can be used to reproduce it.

follows:

$$\begin{aligned}\vec{\tau}_1 &= a(0, 0) \\ \vec{\tau}_2 &= a(1, 1)\end{aligned}\tag{2.1}$$

While defining the basis vectors you are free to place the origin at any point within the unit cell. In this example, the origin is placed at the lower left corner of the unit cell, coinciding with a point. An equally legitimate choice would be to place the origin at the middle of the unit cell.

A more realistic example is displayed in Fig. 2.2. The black and white dots represent two different species. As such, these could be B and N atoms respectively that form a hexagonal BN-sheet. Using one of the equivalent unit cells (hashed area) and combinations of the unit vectors, \vec{a}_1 and \vec{a}_2 , we can generate the entire lattice. Here the lattice and basis vectors are:

$$\begin{aligned}\vec{a}_1 &= a \left(\frac{3}{2}, \frac{\sqrt{3}}{2} \right) & \vec{a}_2 &= a \left(\frac{3}{2}, -\frac{\sqrt{3}}{2} \right) \\ \vec{\tau}_1 &= a \left(\frac{1}{2}, \frac{\sqrt{3}}{2} \right) & \vec{\tau}_2 &= a \left(-\frac{1}{2}, \frac{\sqrt{3}}{2} \right)\end{aligned}\tag{2.2}$$

In Eq. 2.2, a is the length of the B-N bond. In summary, in order to completely specify a crystal, two elements are needed.

1. **Lattice vectors:** Up to three vectors that define the periodic array of unit cells.
2. **Basis vectors:** An arbitrary number of vectors that populate each of the unit cell.

As mentioned previously, a Bravais lattice refers to the lattice generated by the periodic repetition of a single point using arbitrary linear combinations of the lattice vectors. A general translational vector in a periodic lattice can be written as the sum of integer multiples of unit vectors,

$$\vec{T}(\vec{n}) = \vec{T}(n_1, n_2, n_3) = n_1\vec{a}_1 + n_2\vec{a}_2 + n_3\vec{a}_3\tag{2.3}$$

where the three unit vectors \vec{a}_i need not be orthonormal. In fact, in Fig. 2.2, we see that the two unit vectors spanning the space are not orthonormal.

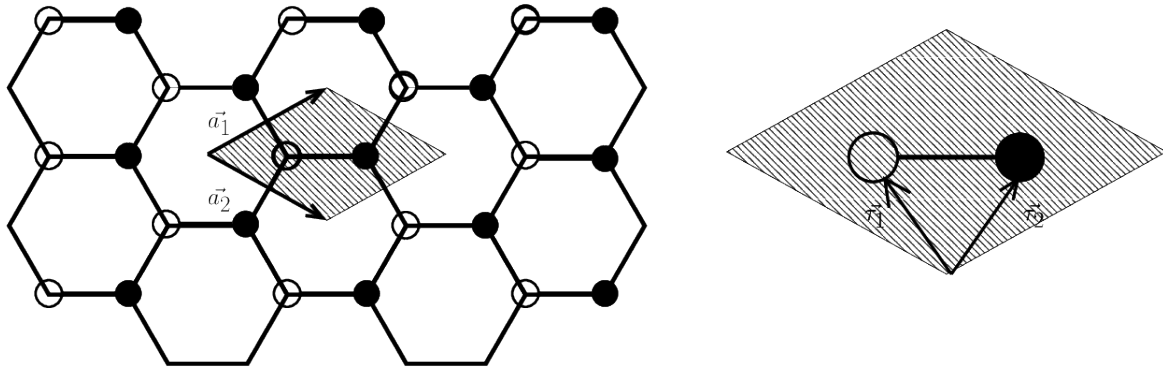


Figure 2.2: Crystal structure of the hexagonal BN sheet.

In three dimensions, there are a total of 14 possible Bravais lattices. Fig. 2.3 displays all possibilities. The lattices are characterized by six properties: the lengths of the three vectors and the angles between them (α, β, γ). The simplest lattice is cubic ($|\vec{a}_1| = |\vec{a}_2| = |\vec{a}_3| = a$, $\alpha = \beta = \gamma = 90^\circ$) while the most general is the triclinic ($|\vec{a}_1| \neq |\vec{a}_2| \neq |\vec{a}_3|$, $\alpha \neq \beta \neq \gamma \neq 90^\circ$). If you take a look at the crystal structure of all the elements of the periodic table, you will see that most of the simple metals (Rh, Pt, Fe) and elemental semiconductors (Si, Fe) either have a bcc (body-centered cubic) or an fcc-based structure. In Fig. 2.3, these correspond to the I and F variants of the cubic lattice. The lattice vectors of the primitive unit cells of the bcc and fcc lattices are:

$$\begin{aligned} \text{FCC: } \vec{a}_1 &= a(1, 1, 0) & \vec{a}_2 &= a(0, 1, 1) & \vec{a}_3 &= a(1, 0, 1) \\ \text{BCC: } \vec{a}_1 &= a(-1, 1, 1) & \vec{a}_2 &= a(1, -1, 1) & \vec{a}_3 &= a(1, 1, -1) \end{aligned} \quad (2.4)$$

where a is the side length of the cube that the fcc and bcc structures are based upon.

2.2 Reciprocal space

Crystals present two length scales. The longer length scale has to do with the fact that crystals are obviously finite materials with bounding surfaces. However, for practical purposes, we treat them as infinite systems satisfying specific boundary conditions², which impose periodicity in all three dimensions,

$$\Psi(\vec{r}) = \Psi(\vec{r} + N_1\vec{a}_1) = \Psi(\vec{r} + N_2\vec{a}_2) = \Psi(\vec{r} + N_3\vec{a}_3) \quad (2.5)$$

where N_i are the numbers of unit cells in each of the three directions along the lattice vectors. Such boundary conditions are referred to as *Born-von Karman* boundary conditions.

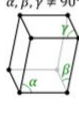
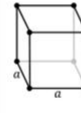

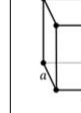
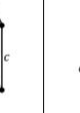
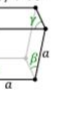

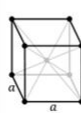

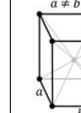


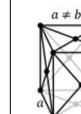
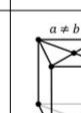

In addition to this long-range periodicity, the crystal has another symmetry on a much shorter scale, namely the lattice vectors. Any function defined for a crystal, such as the electron density, is bound to be periodic, repeating itself with the same translation vectors as those that span the lattice. Thus,

$$f(\vec{r} + \vec{T}(n_1, n_2, n_3)) = f(\vec{r}). \quad (2.6)$$

where $\vec{T} = n_1\vec{a}_1 + n_2\vec{a}_2 + n_3\vec{a}_3$ is a translation vector. It is worth mentioning that while the larger scale periodicity is artificial and imposed by us for convenience, the short length scale is natural and innate to the crystal.

²This is a good approximation unless the system size is so small that surface effects cannot be neglected.

Bravais lattice in 3D (14-types)

	Triclinic	Cubic	Tetragonal	Orthorhombic	Rhombohedral	Hexagonal	Monoclinic
P	$\alpha, \beta, \gamma \neq 90^\circ$ 		$a \neq c$ 	$a \neq b \neq c$ 	$\alpha, \beta, \gamma \neq 90^\circ$ 	$a \neq c$ 	$\alpha \neq 90^\circ$ $\beta, \gamma = 90^\circ$ 
I			$a \neq c$ 	$a \neq b \neq c$ 			
F				$a \neq b \neq c$ 			
C				$a \neq b \neq c$ 			$\alpha \neq 90^\circ$ $\beta, \gamma = 90^\circ$ 

Alam ECE-606 S08 23

Figure 2.3: All 14 Bravais lattices in three dimensions.

Periodic functions such as those mentioned above lend themselves easily to Fourier transform. Under certain conditions, it becomes more advantageous to deal with the Fourier components of such systems rather than dealing with them in real space. The forward Fourier transform is conventionally defined as

$$f(\vec{q}) = \frac{1}{\Omega_{\text{crystal}}} \int_{\Omega_{\text{crystal}}} d\vec{r} f(\vec{r}) \exp(i\vec{q} \cdot \vec{r}). \quad (2.7)$$

where Ω_{crystal} is the volume of the crystal. The Born-von Karman conditions set constraints on the allowed wavevectors, \vec{q} , which we may use while determining the Fourier components. This may easily be seen by adding a translation vector, $N_i \vec{a}_i$ ($i = 1, 2, 3$) to \vec{r} in Eq. 2.5 and making use of Eq. 2.7. For now let us do this along one dimension only:

$$\begin{aligned} f(\vec{q}) &= \frac{1}{\Omega_{\text{crystal}}} \int_{\Omega_{\text{crystal}}} d\vec{r} f(\vec{r} + N_1 \vec{a}_1) \exp(i\vec{q} \cdot (\vec{r} + N_1 \vec{a}_1)) \\ &= \frac{\exp(i\vec{q} \cdot (N_1 \vec{a}_1))}{\Omega_{\text{crystal}}} \int_{\Omega_{\text{crystal}}} d\vec{r} f(\vec{r}) \exp(i\vec{q} \cdot \vec{r}) \end{aligned} \quad (2.8)$$

Comparing Eq. 2.7 and Eq. 2.8, we see that $\exp(i\vec{q} \cdot (N_1 \vec{a}_1)) = 1$. The same argument may be applied to the other two relevant directions, yielding the following restriction on the wavevectors \vec{q} .

$$\vec{q} \cdot \vec{a}_i = \frac{2\pi m_i}{N_i} \quad \text{where } m_i = 0, 1, 2, \dots, N_i - 1 \quad (2.9)$$

We thus have the familiar situation that confinement causes the wavevectors to be quantized (remember particle in a box). Next, we make use of the periodicity on the scale of the lattice

constants. Starting again with the Fourier transform over the entire crystal, we then make use of the small-scale periodicity:

$$\begin{aligned}
f(\vec{q}) &= \frac{1}{\Omega_{\text{crystal}}} \int_{\Omega_{\text{crystal}}} d\vec{r} f(\vec{r}) \exp(i\vec{q} \cdot \vec{r}) \\
&= \frac{1}{N_{\text{cell}}} \sum_{n_1, n_2, n_3} \exp[\vec{q} \cdot \vec{T}(n_1, n_2, n_3)] \frac{1}{\Omega_{\text{cell}}} \int_{\Omega_{\text{cell}}} d\vec{r} f(\vec{r} + \vec{T}(n_1, n_2, n_3)) \exp(i\vec{q} \cdot \vec{r}) \\
&= \frac{1}{N_{\text{cell}}} \prod_i \sum_{n_i} \exp[\vec{q} \cdot (n_i \vec{a}_i)] \frac{1}{\Omega_{\text{cell}}} \int d\vec{r} f(\vec{r}) \exp(i\vec{q} \cdot \vec{r}) \tag{2.10}
\end{aligned}$$

where we make use of the fact that the integral over the volume of the crystal can be broken down into integrals of identical unit cells. Consider one of the sums over $\{n_i\}$:

$$\sum_{n_i=0}^{N_i-1} \left(e^{i\vec{q} \cdot \vec{a}_i} \right)^{n_i} = \frac{1 - e^{i\vec{q} \cdot \vec{a}_i N_i}}{1 - e^{i\vec{q} \cdot \vec{a}_i}} \tag{2.11}$$

where the sum of a geometric series has been used. Due to the fact that $\vec{q} \cdot \vec{a}_i = 2\pi(\text{integer})/N_i$, the denominator is zero. Thus, Eq. 2.11 can only be a finite number if and only if

$$e^{i\vec{q} \cdot \vec{a}_i} = 1 \Rightarrow \vec{q} \cdot \vec{a}_i = 2\pi l_i \tag{2.12}$$

where l_i is an integer. Thus, periodicity at this small scale implies a new selection rule for the allowed wavevectors, \vec{q} . The space spanned by the allowed, discrete set of $\{\vec{q}\}$ that satisfy Eq. 2.12 is called the *reciprocal lattice*. They are referred to as a lattice because just like lattice vectors, they define a regular array of atoms with a well-defined periodicity. Any point in the reciprocal lattice can be expressed in terms of a set of minimal set of \vec{q} 's which are defined by

$$\vec{b}_i \cdot \vec{a}_j = 2\pi \delta_{ij}. \tag{2.13}$$

An arbitrary point on the lattice is then given by

$$\vec{G}(m_1, m_2, m_3) = m_1 \vec{b}_1 + m_2 \vec{b}_2 + m_3 \vec{b}_3. \tag{2.14}$$

One way to satisfy Eq. 2.13 is to construct \vec{b}_i 's such that they obey

$$\vec{b}_i = 2\pi \frac{\vec{a}_j \times \vec{a}_k}{\vec{a}_i \cdot (\vec{a}_j \times \vec{a}_k)} \tag{2.15}$$

The term on the denominator is numerically equal to the volume of the unit cell in real space. For each \vec{G} in Eq. 2.14, the Fourier transform of the periodic function can then be written as

$$f(\vec{G}) = \frac{1}{\Omega_{\text{cell}}} \int_{\Omega_{\text{cell}}} d\vec{r} f(\vec{r}) e^{i\vec{G} \cdot \vec{r}}. \tag{2.16}$$

The discretization of the inverse space (k -space) both due to the Born-von Karman boundary conditions and due to the short length scale is illustrated in Fig. 2.4, where the fine mesh of black dots correspond to the allowed \vec{q} (or usually referred to as \vec{k}) vectors and the blue larger mesh demonstrates the reciprocal lattice corresponding to a square lattice in two dimensions. The area highlighted in the right-hand side portion is a sort of unit cell defined in the reciprocal space analogous to the primitive unit cell in real space.

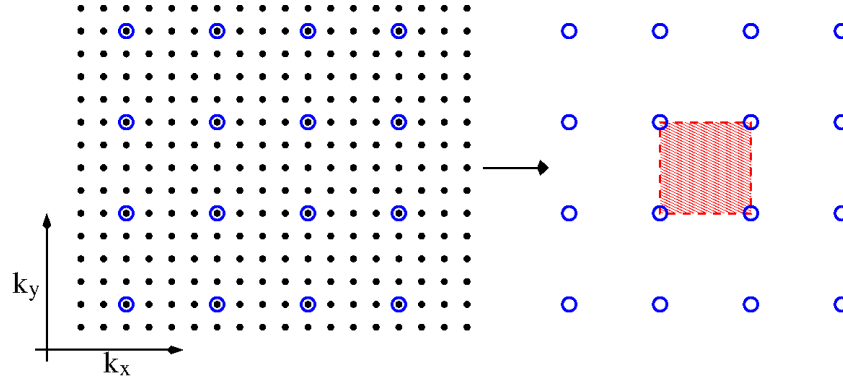


Figure 2.4: Illustration of the discretized k -space and the reciprocal lattice points for a square lattice in two dimensions

2.2.1 An example : Face-centered cubic lattice and its Brillouin zone

A *face-centered cubic* (fcc) lattice is one where the atoms are located on the corners of a cube as well as on the face diagonals. The primitive unit cell is thus given by the following lattice vectors :

$$\begin{aligned}\vec{a}_1 &= a\left(\frac{1}{2}, \frac{1}{2}, 0\right) \\ \vec{a}_2 &= a\left(\frac{1}{2}, 0, \frac{1}{2}\right) \\ \vec{a}_3 &= a\left(0, \frac{1}{2}, \frac{1}{2}\right)\end{aligned}\quad (2.17)$$

Using the definition in Eq. 2.15, we find that the reciprocal lattice vectors are

$$\begin{aligned}\vec{b}_1 &= \frac{2\pi}{a}(1, 1, -1) \\ \vec{b}_2 &= \frac{2\pi}{a}(1, -1, 1) \\ \vec{b}_3 &= \frac{2\pi}{a}(-1, 1, 1)\end{aligned}\quad (2.18)$$

Note that the reciprocal vectors that belong to the fcc lattice define a *body-centered cubic* (bcc) lattice in the reciprocal space.

2.2.2 The Brillouin Zone

From Eq. 2.16, one easily sees that there is a certain periodicity also in the reciprocal space, that is

$$f(\vec{G} + m_i \vec{b}_i) = f(\vec{G}). \quad (2.19)$$

Thus it makes sense to define a *unit cell* also in reciprocal space beyond which f repeats itself. Such a unit cell is already widely used in literature and it is called the *Brillouin zone*. The *Brillouin zone* is defined by the area surrounded by the planes that are perpendicular bisectors of the vectors from the origin to the reciprocal lattice points (see Fig. 2.5). Fig. 2.6 shows an actual three-dimensional example of a Pt crystal, which has an FCC lattice structure and its BCC Brillouin zone.

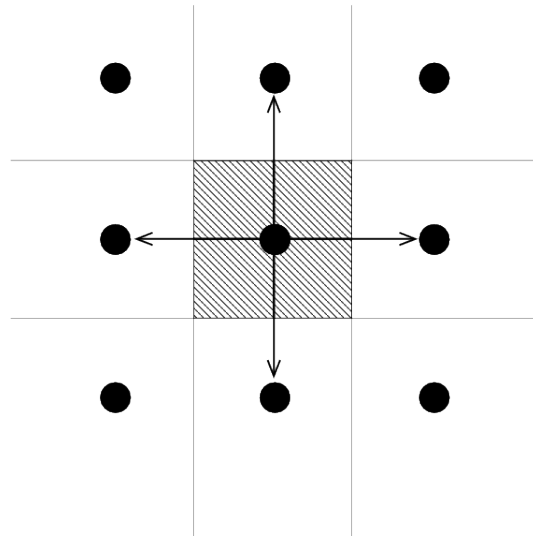


Figure 2.5: Brillouin zone of a square lattice.

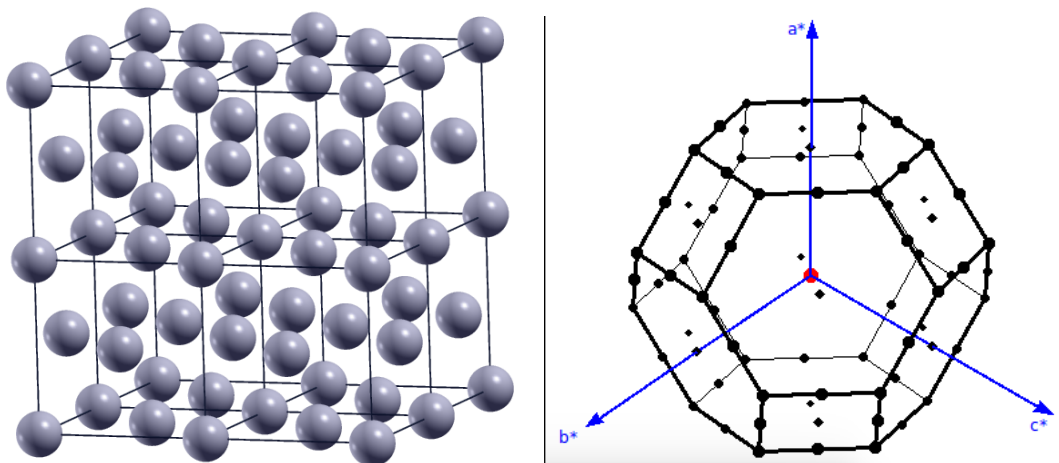


Figure 2.6: Real and reciprocal space of the Pt crystal. The volume delimited on the left is the Brillouin zone.

2.2.3 Bloch's theorem

In a single-electron picture, the Hamiltonian is invariant under lattice translations. Thus the Hamiltonian commutes with the translation operator

$$[\hat{H}, \hat{T}_{\vec{n}}] = 0 \quad \text{where} \quad \hat{T} = \vec{n}_1 \vec{a}_1 + \vec{n}_2 \vec{a}_2 + \vec{n}_3 \vec{a}_3. \quad (2.20)$$

From elementary quantum mechanics, we recall that operators that commute share a common set of eigenfunctions. Such a common set may thus be found also for \hat{H} and $\hat{T}_{\vec{n}}$. Let's consider in particular, $\vec{n}_1 = (1, 0, 0)$. The Born-von Karman conditions require that the eigenfunctions remain unchanged if the translation operator is applied N_1 times

$$\left(\hat{T}_{\vec{n}_1}\right)^{N_1} \psi(\vec{r}) = (t_{\vec{n}_1})^{N_1} \psi(\vec{r}) = \psi(\vec{r}) \quad (2.21)$$

where $t_{\vec{n}_1}$ is the eigenvalue of the translation operator $\hat{T}_{\vec{n}_1} \psi(\vec{r})$. The requirement

$$(t_{\vec{n}_1})^{N_1} = 1 \quad (2.22)$$

is satisfied for e^{ik} where k is, at this point, just a real number. Eq. 2.22, on the other hand, dictates that

$$e^{ikN_1} = 1 \quad \Rightarrow \quad kN_1 = 2\pi n_1 \quad \Rightarrow \quad k = \frac{2\pi n_1}{N_1} \quad (2.23)$$

The same relation may be written by a general k restricted to the first Brillouin zone

$$\vec{k} = \frac{n_1}{N_1} \vec{b}_1 + \frac{n_2}{N_2} \vec{b}_2 + \frac{n_3}{N_3} \vec{b}_3 \quad (2.24)$$

We finally arrive at Bloch's theorem which states that the eigenfunctions of a lattice-periodic Hamiltonian must satisfy

$$\hat{T}_{\vec{n}} \psi(\vec{r}) = e^{i\vec{k} \cdot \vec{T}_{\vec{n}}} \psi(\vec{r}). \quad (2.25)$$

Bloch's theorem states that eigenstates of a periodic Hamiltonian pick up a phase when translated by a translation vector and may thus be labeled by the wavevector that characterizes the phase factor. In particular, Eq. 2.25 is satisfied by wavefunctions that can be written as

$$\psi(\vec{r}) = e^{i\vec{k} \cdot \vec{r}} u_{\vec{k}}(\vec{r}) \quad (2.26)$$

where $u_{\vec{k}}(\vec{r})$ is a lattice periodic function with

$$u_{\vec{k}}(\vec{r} + \vec{T}_{\vec{n}}) = u_{\vec{k}}(\vec{r}). \quad (2.27)$$

Eq. 2.26 is an equivalent statement of Bloch's theorem. This can be proven easily by substituting Eq. 2.26 into Eq. 2.25. Let's illustrate this with the following picture in one dimension as seen in Fig. 2.7. The bottommost line is a lattice periodic wavefunction of period $a = 1$ in some units. The line in the middle is the phase factor e^{ikx} for $k = \pi/2a$ and the topmost curve is the wavefunction that is their product (its real part, to be more precise). As you see, unlike such observables as the electron density, the wavefunction *need not* have the periodicity of the lattice. It is still required however to obey the Born-von Karman boundary conditions.

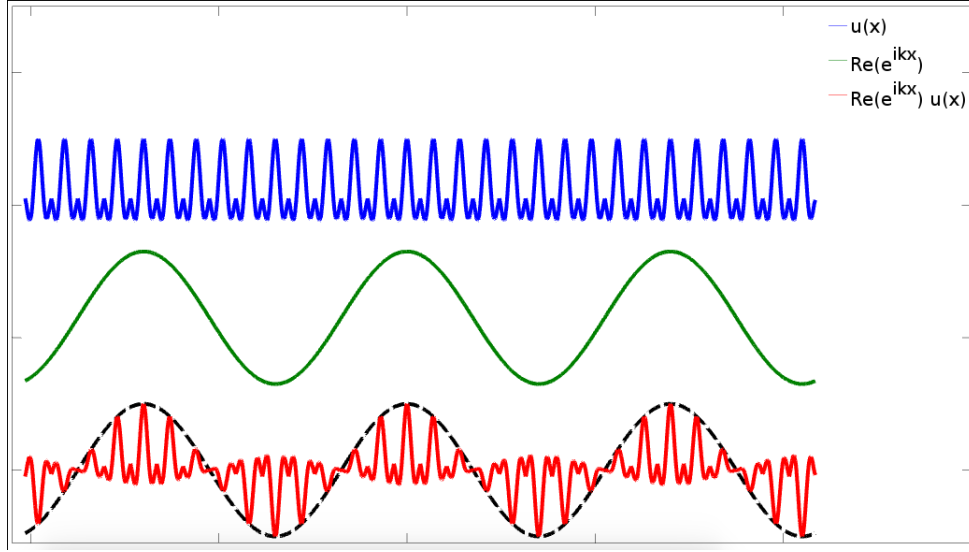


Figure 2.7: Example of a wavefunction that obeys Bloch's theorem.

2.3 Band structure

The ability provided by the Bloch theorem to break down the wavefunction into a lattice-periodic function $u_{\vec{k}}$ and a phase factor allows us to work with a reduced, wavevector-dependent Hamiltonian. Applying the real Hamiltonian \hat{H} of the system on to the wavefunction given in Eq. 2.26, we have³

$$\begin{aligned}\hat{H}\psi_{i,\vec{k}}(\vec{r}) &= \epsilon_{i,\vec{k}}\psi_{i,\vec{k}}(\vec{r}) \\ \hat{H}e^{i\vec{k}\cdot\vec{r}}u_{i,\vec{k}}(\vec{r}) &= \epsilon_{i,\vec{k}}e^{i\vec{k}\cdot\vec{r}}u_{i,\vec{k}}(\vec{r})\end{aligned}\quad (2.28)$$

Multiplying the second line in Eq. 2.28 by $e^{-i\vec{k}\cdot\vec{r}}$, we have

$$\begin{aligned}e^{-i\vec{k}\cdot\vec{r}}\hat{H}e^{i\vec{k}\cdot\vec{r}}u_{i,\vec{k}}(\vec{r}) &= \epsilon_{i,\vec{k}}u_{i,\vec{k}}(\vec{r}) \\ \hat{H}_{\vec{k}}u_{i,\vec{k}}(\vec{r}) &= \epsilon_{i,\vec{k}}u_{i,\vec{k}}(\vec{r})\end{aligned}\quad (2.29)$$

where $\hat{H}_{\vec{k}} = e^{-i\vec{k}\cdot\vec{r}}\hat{H}e^{i\vec{k}\cdot\vec{r}}$. It is therefore possible to scan the Brillouin zone by writing and solving a new Hamiltonian for each wavevector. Each $\hat{H}_{\vec{k}}$ will yield a spectrum of eigenvalues and in the limit of large crystal dimension, these eigenvalues will merge into a continuous graphical representation of eigenvalues, which is called the *band structure*. The band structure is a very important tool for deciding upon the electronic properties of a crystal.

2.3.1 The Krönig-Penney model

The Krönig-Penney (KP) model is an overly idealized description of a one dimensional crystal that, however, illustrates the band structure rather well. In the KP model, the nuclei are represented by a periodic array of wells with width b and separated by a length a (see Fig. 2.8. The true nuclear potential that a single electron sees is Coulombic and looks similar to

³The new index i designates each eigenfunction in the spectrum of a given \vec{k}

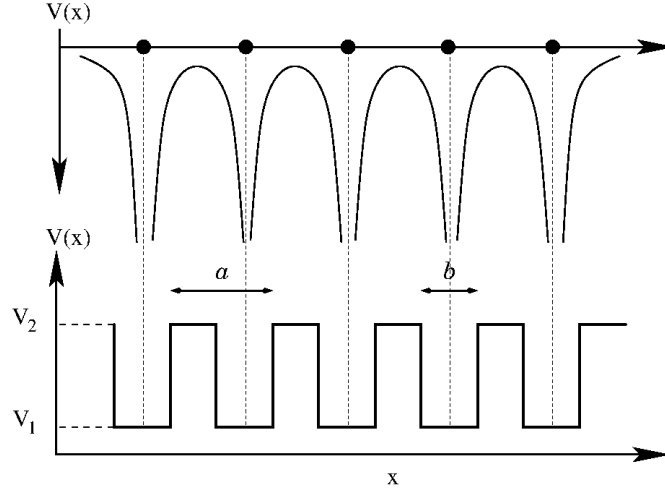


Figure 2.8: The Krönig-Penney Model. The true nuclear potential (upper panel) and the approximation (lower panel).

the sketch on the top panel of Fig. 2.8. However, due to screening by other electrons, each electron sees a much less strongly negative potential. The KP model takes advantage of this fact to represent the finite nuclear barriers as regions with a constant potential, which is taken to be zero⁴. In the region between the wells, the potential is taken to be V_0 . Once the model is established, we utilize the method develop for the finite barrier. The solutions in the wells must be sinusoidal while those in the inbetween region, must be exponential. However, this time, the external solutions are not required to decay therefore we are required to consider both the growing and decaying solutions. First let us consider the solutions in the interval $-L < x < b$. The solutions, in this interval, have the general form

$$\begin{aligned}\psi_I(x) &= Ae^{iqx} + Be^{-iqx} & -L < x < 0 \\ \psi_{II}(x) &= Ce^{\beta x} + De^{-\beta x} & 0 < x < b.\end{aligned}\quad (2.30)$$

With the wave functions as defined, the energies are

$$\begin{aligned}E_I &= \frac{\hbar^2 q^2}{2m} \\ E_{II} &= V_0 - \frac{\hbar^2 \beta^2}{2m},\end{aligned}\quad (2.31)$$

similar to the barrier problem. Once again, we need to find the four arbitrary constant through boundary conditions. However, this time, we have infinitely many boundaries at which to match the solutions. Instead of doing that, we utilize the Bloch theorem:

$$\begin{aligned}\psi_I(0) = \psi_{II}(0) &\Rightarrow A + B = C + D \\ \psi'_I(0) = \psi'_{II}(0) &\Rightarrow Aiq - Biq = C\beta - D\beta \\ \psi_{II}(b) = e^{ika}\psi_I(-L) &\Rightarrow Ce^{\beta b} + De^{\beta b} = e^{ika} [Ae^{-iqL} + Be^{iqL}] \\ \psi'_{II}(b) = e^{ika}\psi'_I(-L) &\Rightarrow C\beta e^{\beta b} - De^{-\beta b} = e^{ika} [Aiqe^{-iqL} - Biqe^{iqL}]\end{aligned}\quad (2.32)$$

⁴As the reference point of energy is arbitrary, you can take this to be anything you want

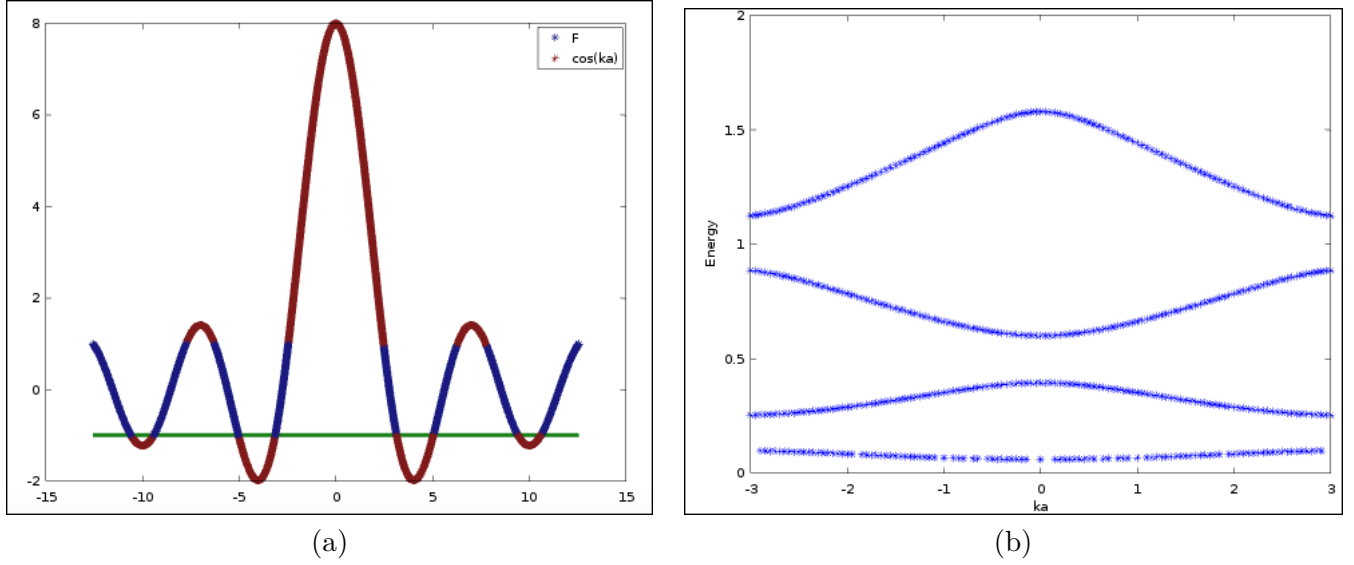


Figure 2.9: The forbidden (red) and allowed (blue) energy values of the Krönig-Penney model (a). The horizontal line corresponds to $\cos(ka) = 0$. The band structure is also shown (b), which corresponds to the intersection points of function on the right and the horizontal line.

In the third and fourth equations in Eq. 2.32, the match is really between the region where $x < b$ and $x > b$. However, Bloch's theorem states that $\psi(b) = e^{ika}\psi(-L)$.

The system of equations in Eq. 2.32 have nontrivial solutions only if the determinant of coefficients that multiple A, B, C and D is zero. Writing down this determinant and solving (which shall be left to the reader as an exercise) yields:

$$\frac{\beta^2 - q^2}{2qL} \sinh(\beta b) \sin(qL) + \cosh(\beta b) \cos(qL) = \cos(ka) \quad (2.33)$$

One immediately notices that solutions do not exist for every value of q and β or in other words for every value of E . As $-1 \geq \cos(ka) \leq 1$ Those E values that do not satisfy

$$|f(q)| \equiv \left| \frac{\beta^2 - q^2}{2qL} \sinh(\beta b) \sin(qL) + \cosh(\beta b) \cos(qL) \right| \leq 1 \quad (2.34)$$

are *forbidden*. Eq. 2.33 can be solved numerically by means of plotting the function $f(q)$ and $\cos(ka)$ as in Fig. 2.3.1(a) and finding the intersection points. For each value of k in the Brillouin zone, there are infinitely many energy values, but only the lowest of these values are of practical concern. Once we plot these energies together in a single graph, we obtain the band structure for the Krönig-Penney model (see Fig. 2.3.1).

$$P \frac{\sin(qa)}{qa} + \cos(qa) = \cos(ka) \quad (2.35)$$

where $P = \frac{mV_0ba}{\hbar^2}$. One feature that is immediately noticeable is the lack of allowed states for certain values of k . These gaps are called *band gaps* and are very important in understanding important physical properties of materials. For instance, if the Fermi energy falls within a band gap, the structure is a semiconductor but if it intersects a band, we have a metal.

2.3.2 The tight-binding approximation

A model that goes one large step beyond the KP model while still remaining simple enough is the *tight-binding model*. This model takes into account the particular chemical properties of the atoms making up the crystal instead of treating all nuclei uniformly as finite potential wells. In order to illustrate the main idea, we have introduced above, let's see a very simple one-dimensional example⁵. Assume that we have a one-dimensional arrangement of infinitely many atoms on a chain and assume Born-von Karman boundary conditions with a period of N atoms.

We are going to employ what is known as the *tight-binding model* where the variational wavefunction is an expansion in terms of atomic orbitals located on different atoms. The character of orbitals to be included in the expansion depends on the species included. For a carbon chain, for instance, it is usually sufficient to take the $2s$ and the $2p$ orbitals since the $1s$ orbitals do not contribute to bonding. However, here we shall only consider the $1s$ orbitals to illustrate the idea.

Let us go through the steps of the calculations one by one :

1. Start with the atomic orbitals centered on each atom :

$$\phi_l(x - na) \quad (2.36)$$

where l is the orbital label (in three dimensions, $l = 2s, 2p_x, 2p_y, 2p_z$ etc.), x is the coordinate variable, na is the location of the n th atom and a is the lattice constant.

2. Construct k -dependent functions from the orbitals in Eq. 2.36 to be used as a basis.

$$\chi_{kl}(x) = \frac{1}{\sqrt{N}} \sum_n e^{ikna} \phi_l(x - na) \quad (2.37)$$

where N is the number of atoms in the Born-von Karman cell. The normalization constant should be self-explanatory.

3. Check to make sure that χ_{kl} obey Bloch's theorem.

$$\chi_{kl}(x + n'a) = \frac{1}{\sqrt{N}} \sum_n e^{ikna} \phi_l(x - (n - n')a) \quad (2.38)$$

Define a new variable for the summation $n'' = n - n'$ and substitute into Eq. 2.38.

$$\begin{aligned} \chi_{kl}(x + n'a) &= \frac{1}{\sqrt{N}} \sum_{n''} e^{ik(n'+n'')a} \phi_l(x - n''a) \\ &= \frac{1}{\sqrt{N}} e^{ikn'a} \sum_{n''} e^{ikn''a} \phi_l(x - n''a) \\ &= e^{ikn'a} \chi_{kl}(x). \end{aligned} \quad (2.39)$$

4. Construct the variational wavefunction — do not forget that k is a good quantum number for this wavefunction.

$$\Psi_k(x) = \sum_l c_{kl} \chi_{kl}(x) = \sum_{ln} c_{kl} e^{ikna} \phi_l(x - na) \quad (2.40)$$

⁵Adapted from the book by Kaxiras

5. Construct the variational equations to find the coefficients

$$\sum_{lm} \left[\langle \chi_{km} | \hat{H} | \chi_{kl} \rangle - \varepsilon_k \langle \chi_{km} | \chi_{kl} \rangle \right] c_{kl} = 0 \quad (2.41)$$

6. Look at the overlap term in Eq. 2.41. Substitute Eq. 2.37 :

$$\begin{aligned} \langle \chi_{kl} | \chi_{km} \rangle &= \frac{1}{N} \sum_{nn'} e^{ik(n-n')a} \langle \phi_l(na) | \phi_m(n'a) \rangle \\ &= \frac{1}{N} \sum_{nn'} e^{ik(n-n')a} \langle \phi_l(0) | \phi_m(na - n'a) \rangle \end{aligned} \quad (2.42)$$

where $|\phi_m(na)\rangle$ refers to an orbital centered on the n th atom located at $x = na$. Now let $n'' = n - n'$

$$\begin{aligned} \langle \chi_{kl} | \chi_{km} \rangle &= \frac{1}{N} \sum_{n'n''} e^{ikn''a} \langle \phi_l(0) | \phi_m(n''a) \rangle \\ &= \sum_n e^{ikna} \langle \phi_l(0) | \phi_m(na) \rangle \end{aligned} \quad (2.43)$$

Eq. 2.43 is the most general expression for a general set of orbitals. In this simple example, we only consider one kind of orbital, namely $l = 1s$ and as a result the sum over l in Eq. 2.43 reduces to a single term.

Next, we assume that the overlap between the orbitals on neighboring atoms is so small that the inner product of orbitals in Eq. 2.43 is nonzero only when $n = 0$, i.e. when both orbitals are on the same atom. This is not necessary but makes our job easier. Thus,

$$\langle \phi(0) | \phi(na) \rangle = \delta_{n,0} \quad (2.44)$$

7. Similarly for the matrix element of the Hamiltonian,

$$\langle \chi_{kl} | \hat{H} | \chi_{km} \rangle = \sum_n e^{ikna} \langle \phi(0) | \hat{H} | \phi(na) \rangle \quad (2.45)$$

This time, we assume that the Hamiltonian matrix element does not only remain on-site but extends to neighbors. This amounts to

$$\langle \phi(0) | \hat{H} | \phi(na) \rangle = \varepsilon_s \delta_{n,0} + t \delta_{n,\mp 1}. \quad (2.46)$$

This particular approximation is referred as the *nearest-neighbor approximation*.

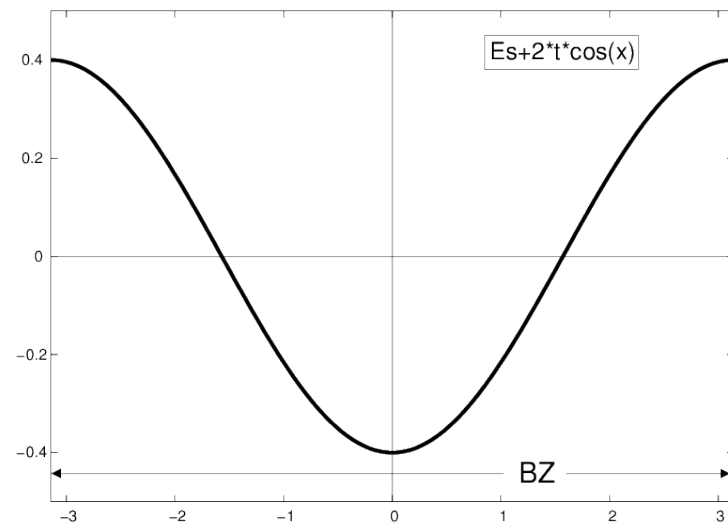
8. Substitute Eq. 2.44 and Eq. 2.46 into Eq. 2.41 to get

$$\sum_n e^{ikna} (\varepsilon_s \delta_{n,0} + t \delta_{n,\mp 1}) = \varepsilon_k \sum_n e^{ikna} \delta_{n,0}. \quad (2.47)$$

Note that even though the original equation started out as a matrix equation to determine the coefficients, the simplicity of the single-orbital assumption turned it into a single equation.

9. Finally, we obtain the following analytic equation for the energy eigenvalues

$$\varepsilon_k = \varepsilon_s + 2t \cos ka \quad (2.48)$$



3

The concept of confinement

In this chapter we are going to look at examples of confinement in 2, 1 and 0 dimensions. We shall see that each time confinement is imposed in a given direction, the energy levels associated with that direction are quantized. For the examples we shall see the Schrödinger equation in each direction may be separated. Thus, we may conveniently treat the problem in each dimension as a separate system.

3.1 Density of free-particle states in three, two and one dimensions

An important function in determining important properties of devices such as conductance is the *density of states*. Density of states (DOS) is a measure of *number of states in an infinitesimal energy window between E and $E + dE$* . If we represent this number of states by dN , then we may then relate dN and dE through

$$dN = \rho(E)dE \quad \Rightarrow \quad \rho(E) = \frac{dN}{dE}. \quad (3.1)$$

where $\rho(E)$ is the density of states. Note that density of states is meant to describe *the number of states per energy per unit volume, area or length of the system*. Let us now concentrate on a three-dimensional semiconductor described by the effective mass approximation. The energy is then related to the wavevector through the relation

$$E(\vec{k}) = \frac{\hbar^2 k^2}{2m^*} \quad (3.2)$$

where k is the norm of the wavevector \vec{k} . The form of the energy is always the same in all three dimensions. What changes and what makes the density of states different is the number of states in a given volume in the reciprocal space. The number of states $N(E)$ per volume for a given energy E can be thought of as the number of wavevectors that fall into a sphere in reciprocal space with a radius k_{max} corresponding to the energy E . Another way to see this is through calculating the “volume” associated with each wavevector in the reciprocal space. As we have seen before, the momenta of the free-electron states are thought to be quantized in all three directions in the reciprocal space in intervals of $\Delta k_x = \frac{2\pi}{L_x}$, $\Delta k_y = \frac{2\pi}{L_y}$ and $\Delta k_z = \frac{2\pi}{L_z}$. Thus the volume in reciprocal space associated with a momentum state is given by

$$\Delta V = \frac{(2\pi)^3}{L_x L_y L_z} = \frac{(2\pi)^3}{V} \quad (3.3)$$

where V is the volume of the Born-von Karman box in real space. For a given energy, $E = \hbar k^2/2m^*$, the volume of a sphere of radius k in three dimensions is

$$V(E) = \frac{4\pi}{3}k^3. \quad (3.4)$$

and the number of states within this volume is

$$\frac{V(E)}{\Delta V} = \frac{\frac{4\pi}{3}k^3}{\frac{(2\pi)^3}{V}} = \frac{Vk^3}{6\pi^2}. \quad (3.5)$$

However, the final expression in Eq. 3.5 contains the volume of the system and is therefore *extensive*. In order to make it *intensive* we divide by the volume of the system reaching our goal of calculating the number of states at a given energy per unit volume in real space,

$$N(E) = \frac{k^3}{6\pi^2} = E^{3/2} \left(\frac{\sqrt{2m^*}}{\hbar} \right)^3 \frac{1}{6\pi^2} \quad (3.6)$$

where the final expression is achieved by converting the wavevector to energy. Finally, the density of states in three dimensions is given by

$$\rho_{3D} = \frac{dN}{dE} = \frac{1}{4\pi^2} \left(\frac{\sqrt{2m^*}}{\hbar} \right)^3 E^{1/2}. \quad (3.7)$$

In two and one-dimensions, the discussion is analogous except the number of states in Eq. 3.5. In two dimensions the “volume” (really area) in reciprocal with a radius k is given by

$$A(E) = 4\pi k^2, \quad (3.8)$$

the area associated with each state is

$$\Delta A = \frac{(2\pi)^2}{A} \quad (3.9)$$

and finally the number of states for energy E per unit volume in real space is

$$N(E) = \frac{k^2}{\pi} = \frac{2m^*}{\pi\hbar^2}E. \quad (3.10)$$

The density of states in two dimensions is then

$$\rho_{2D}(E) = \frac{dN}{dE} = \frac{2m^*}{\pi\hbar^2}. \quad (3.11)$$

Eq. 3.11 indicates the rather surprising fact that the density of states in two dimensions is independent of the energy E . This is in contrast to the other dimensionalities.

Finally the one-dimensional case is entirely analogous to the previous derivations and the end result is

$$\rho_{1D}(E) = \frac{2m^*}{\hbar}E^{-1/2}. \quad (3.12)$$

The derivations we have gone through in this section refer to systems that are ideally three, two and one dimensional. In the following sections we will see the density of states of systems that are more realistic and therefore not exactly two or one-dimensional but are *confined* in some of the dimensions.

3.2 2-dimensional confinement — 2-dimensional electron gas

Remember the superlattice problem considered in the previous section. Between the two materials to either side of the interface, a potential well is formed that traps electrons in an essentially 2-dimensional configuration. Thus, along perpendicular to the interface, the system is a one dimensional particle in a box, the other two dimensions, however, are perfectly free. Assuming that the confinement occurs in the z direction, the problem in the xy -plane reduces to a free-electron system. The Schrödinger equation then has the following form

$$\left\{ -\frac{\hbar^2}{2m} \left[\frac{\partial^2}{\partial x^2} + \frac{\partial^2}{\partial y^2} \right] + V(z) \right\} \Psi(x, y, z) = E\Psi(x, y, z) \quad (3.13)$$

where

$$V(z) = \begin{cases} 0 & 0 < z < L \\ \infty & \text{elsewhere} \end{cases} \quad (3.14)$$

for a confinement length of L along the z -direction. The potential on the xy -plane on the other hand is zero. In such cases where the problem can be thought of as three independent systems the Schrödinger equation in Eq. 3.13 is said to be *seperable*. The wavefunction $\Psi(x, y, z)$ may be written as a product of three functions each in a separate direction

$$\Psi(x, y, z) = \psi_x(x)\psi_y(y)\psi_z(z). \quad (3.15)$$

Substituting Eq. 3.15 into Eq. 3.13 yields

$$\left\{ -\frac{\hbar^2}{2m} \left[\frac{\partial^2}{\partial x^2} \psi(x)\psi(y)\psi(z) + \frac{\partial^2}{\partial y^2} \psi(y)\psi(x)\psi(z) \right] + V(z)\psi(z)\psi(x)\psi(y) \right\} \Psi(x, y, z) = E\psi(x)\psi(y)\psi(z). \quad (3.16)$$

Dividing Eq. 3.16 by $\psi(x)\psi(y)\psi(z)$ ¹ one obtains

$$-\frac{\hbar^2}{2m} \left\{ \frac{\frac{\partial^2}{\partial x^2} \psi(x)}{\psi(x)} + \frac{\frac{\partial^2}{\partial y^2} \psi(y)}{\psi(y)} \right\} + \frac{V(z)\psi(z)}{\psi(z)} = E \quad (3.17)$$

which is to be satisfied for each and every value of x , y and z . Since each term is a function of one variable only, the only way this can be satisfied is if each of the three terms *independently* equal a constant. In other words, instead of a single Schrödinger equation we deal with three.

$$-\frac{\hbar^2}{2m} \frac{\partial^2}{\partial x^2} \psi(x) = E_x \psi(x) \quad (3.18)$$

$$-\frac{\hbar^2}{2m} \frac{\partial^2}{\partial y^2} \psi(y) = E_y \psi(y) \quad (3.19)$$

$$V(z)\psi(z) = E_z \psi(z). \quad (3.20)$$

where $E = E_x + E_y + E_z$. We immediately recognize Eq. 3.18 and Eq. 3.19 as free particle Schrödinger equations with solutions

$$\psi(x) = \frac{1}{\sqrt{L_x}} e^{ik_x x} \quad (3.21)$$

$$\psi(y) = \frac{1}{\sqrt{L_y}} e^{ik_y y} \quad (3.22)$$

¹Here we assume, without loss of too much generality that the division does not result in divergences.

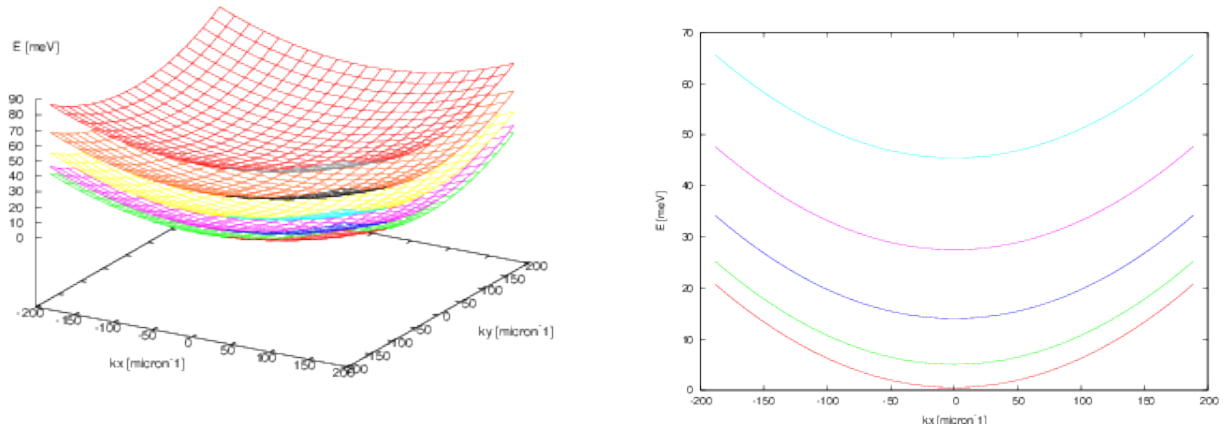


Figure 3.1: Subbands in a two-dimensional system of free particles

with free-particle energies $E_{x,y} = \frac{\hbar^2 k_{x,y}^2}{2m^*}$. The solutions to Eq. 3.20 are simply the particle-in-a-box states

$$\psi(z) = \sqrt{\frac{2}{L_z}} \sin k_z z \quad \text{with} \quad k_z = \frac{n_z \pi}{L_z} \quad (3.23)$$

and the energies are $E_{n_z} = \frac{\hbar^2 \pi^2 n_z^2}{2m^* L_z^2}$. To sum up, the energy levels of the confined system are

$$E(k_x, k_y, n_z) = \frac{\hbar^2 k_x^2}{2m^*} + \frac{\hbar^2 k_y^2}{2m^*} + \frac{\hbar^2 \pi^2 n_z^2}{2m^* L_z^2}. \quad (3.24)$$

In order to contrast the confined system to an ideal two-dimensional system, let us go back to the density of states discussed in the previous section. In a two-dimensional system, density of states was shown to be independent of energy and is given by

$$\rho_{2D}(E) = \frac{m^*}{\pi \hbar^2}. \quad (3.25)$$

In a system confined to two-dimensions, each value of n_z may be thought to yield a different free-particle system with all energies shifted by E_{n_z} . In Fig. 3.1 the energy levels of such a system are shown. The figure on the right is a two-dimensional cut along the $k_y = 0$ plane. Starting at $E = 0$ and cranking up the energy values, we initially observe no density of states until $E = E_0$. Between $E = E_0$ and $E = E_1$, there is only one dispersion curve and thus the system acts like a regular two-dimensional electron gas. When $E = E_1$, however an extra dispersion curve provides an additional channel and the density of states in the interval between $E = E_1$ and $E = E_2$ should be multiplied by two. Similarly between $E = E_2$ and $E = E_3$ a third dispersion curve starts to contribute to the number of available states. As a result, every time a new dispersion curve is added there is a jump in the density of states of the system. Then the new density of states may be written as

$$\rho_{2D}(E) = \sum_{n=1}^{\infty} \Theta(E - E_n) \frac{m^*}{\pi \hbar^2} \quad (3.26)$$

which is simply a collection of steps of equal height but varying width as seen in Fig. 3.2. The channels that are available for electron occupation is termed *subbands*. For instance, between $E = E_i$ and $E = E_{i+1}$ there are i subbands.

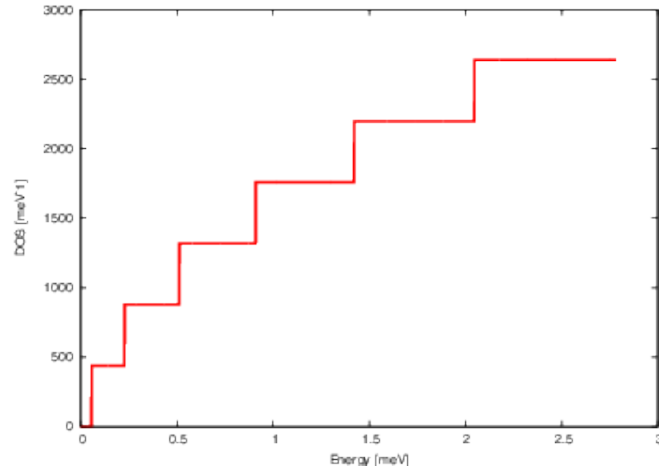


Figure 3.2: DOS of a two-dimensional system of free particles

3.3 1-dimensional confinement — Nanowires

The treatment of one and zero dimensional confinement is analogous to the two-dimensional case. In systems confined in a single dimension such as nanowires, the free electron description is valid for only one dimension. In the simplest case, the confinement in the other two dimensions may be described by the particle in a box². The separation of variables in the Schrödinger equation is done completely analogously. Assuming free-electron-like behavior along the z -direction, the energy levels in this case are given by

$$E_{k_x, n_y, n_z} = \frac{\hbar^2 k_x^2}{2m^*} + \frac{\hbar^2 \pi^2 n_y^2}{2m^* L_y^2} + \frac{\hbar^2 \pi^2 n_z^2}{2m^* L_z^2}. \quad (3.27)$$

In this case, the contribution to the one-dimensional DOS from each subband has a more complicated structure since each discrete energy associated with the box states have an additional degeneracy due to the quantum numbers n_y and n_z . For $n_y = n_z$, the degeneracy of the energy state is 1 since there is only one such alternative. However for $n_y \neq n_z$, there are two identical situations for each level. For instance, the state with $n_y = 1, n_z = 2$ has the same energy as the case $n_y = 2, n_z = 1$. Thus, all such states are doubly degenerate.

The density of states is then

$$\rho_{1D} = \sum_{n_x=1}^{N_x} \sum_{N_y}^{\infty} \frac{2m^*}{\hbar^2} g_{n_x, n_y} \frac{1}{\pi(E - E_{n_x, n_y})} \times \Theta(E - E_{n_x, n_y}) \quad (3.28)$$

where g_{n_x, n_y} is the degeneracy of the particular level taking the values one or two, N_x and N_y are the quantum numbers of the highest confined state in the box. As seen in the figure to the right, the density of states has the same overall structure as in the two-dimensional case with increasing steps, but of course a very different functional dependence.

²Of course, depending on the real system this confinement may be described by other models such as the harmonic oscillator potential, circular box and the triangular potential.

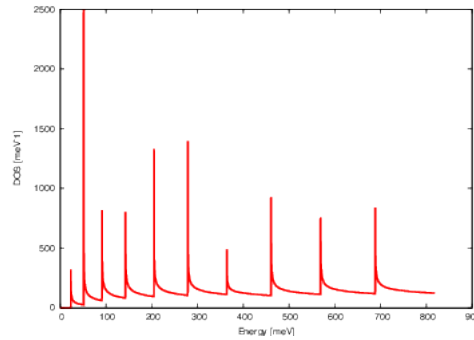


Figure 3.3: Density of states of a one-dimensional system

3.4 0-dimensional confinement — Quantum dots

Finally, in the zero-dimensional case, i.e. confinement in all three directions, there are not free-particle-like states and thus, density of states essentially becomes a collection of sharp peaks³. The energy levels are now characterised by three integers and are given by

$$E_{n_x, n_y, n_z} = \frac{\hbar^2 \pi^2}{2m^*} \left(\frac{n_x^2}{L_x^2} + \frac{n_y^2}{L_y^2} + \frac{n_z^2}{L_z^2} \right) \quad (3.29)$$

and the corresponding density of states is then

$$\rho_{1D}(E) = \sum_{n_x}^{N_x} \sum_{n_y}^{N_y} \sum_{n_z}^{N_z} \Theta(E - E_{n_x, n_y, n_z}) g_{n_x, n_y, n_z} \quad (3.30)$$

where g_{n_x, n_y, n_z} is the degeneracy of each energy level. The degeneracy of levels in the 3-dimensional case is slightly more complicated than the previous case. For a given triplet of (n_x, n_y, n_z) values there are three cases: when all three numbers are the same, when all three are different and when only two of the three numbers are the same. When all three numbers are different there are $3!$ different permutations one can achieve. If all are the same there is only one possibility and if only two are the same, then the remaining number may be placed in three different locations and thus the number of possibilities is 3. In summary, the degeneracy factor may be written as

$$g_{n_x, n_y, n_z} = \begin{cases} 3! & n_x \neq n_y \neq n_z \\ 3 & \text{if two of the indices are the same} \\ 1 & n_x = n_y = n_z \end{cases} \quad (3.31)$$

3.5 A different manifestation of confinement — graphene and nanotubes

In this section, we shall see a completely different sort of confinement with very similar consequences. The systems we studied so far were reduced dimensionality versions of semiconductor heterostructures that may be described in the free dimension with a free-electron-like model. However, there are many systems in the nanoscale where the electron behavior is rather different

³This of course refers to the rectangular box approximation. Other models such as the spherical dot may also be considered.

from the free-electron. This means that the shape of the bands in the band structure deviates substantially from a parabola.

Graphite is a three-dimensional structure that is made up of alternating layers of graphene. Graphene, in turn, is a hexagonal network of carbon atoms and has a *semimetallic character*. This means that the band structure of graphene cannot be easily described in the effective mass approximation and that the density of states of a free electron cannot be used. Instead a simple theory has been devised in order to describe bonding between carbon atoms and many other species called the *tight-binding approximation*. In this approximation, the interaction between only the neighboring atoms are taken into account and is parameterized in a simplified manner.

A carbon atom has 6 electrons, 2 of which belong to the 1s state and therefore have no effect on binding. The other four electrons distributed between the 2s and 2p electrons on the other hand interact with each other and give rise to covalent bonding. Thus, each C atom in a graphene network has four electrons available for bonding. If we expand the wavefunction of the entire system in terms of these orbitals located on all the atoms in our graphene crystal, we have

$$\Psi(\vec{r}) = \sum_A \sum_{n=2s,2p_x,2p_y,2p_z} C_{A,n} \phi_n(\vec{r} - \vec{r}_A). \quad (3.32)$$

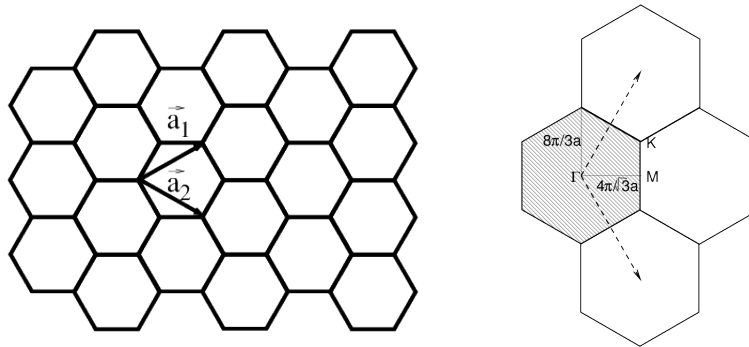
where n runs over atomic orbitals centered on the various atoms in the crystal and A runs over atomic positions. Finding the expectation value is then nothing but writing down a large matrix of expectation values between these orbitals and then solving this matrix equation.

$$h_{An,Bm} = \langle \phi_{A,n} | \hat{H} | \psi_{B,m} \rangle \quad (3.33)$$

In order to make the calculation of such matrix elements easier, one makes several approximations :

1. Only nearest neighbors interact.
2. Electrons do not interact with each other. In other words, this is a single-particle problem.
3. The interaction between neighboring atoms depend on the distance between the atoms and the relative angle that the orbitals make. Of course, this applies only to p orbitals since s orbitals are spherical.

The real space arrangement of atoms in graphene are as seen in the figure below. The Brillouin zone as discussed in previous lectures is given to the right.



The lattice vectors, \vec{a}_1 and \vec{a}_2 are

$$\begin{aligned} \vec{a}_1 &= a \left(\frac{\sqrt{3}}{2}, \frac{1}{2} \right) \\ \vec{a}_2 &= a \left(\frac{\sqrt{3}}{2}, -\frac{1}{2} \right) \end{aligned} \quad (3.34)$$

where a is the length of the unit cell (which is $\sqrt{3}$ times the C-C bond length) in graphene and the corresponding reciprocal lattice vectors are

$$\begin{aligned}\vec{b}_1 &= \frac{2\pi}{a} \left(\frac{1}{\sqrt{3}}, 1 \right) \\ \vec{b}_2 &= \frac{2\pi}{a} \left(\frac{1}{\sqrt{3}}, -1 \right)\end{aligned}\tag{3.35}$$

which may easily be checked. The Brillouin zone in this case is once again a hexagon as seen in the figure above on the right hand side but it is rotated with respect to the real space unit cell by 60° . The special points labeled in the Brillouin zone are high symmetry points and band structure of graphene is usually drawn following lines between these high symmetry points. Using the tight-binding formalism, one can easily calculate the band structure for particular k -values. In particular we concentrate on the π bands since the energy levels which are active in conduction comes from these bands. Solving the tight-binding secular equation for these bands for a generic wavevector $\vec{k} = (k_x, k_y)$, the energy levels come out to be

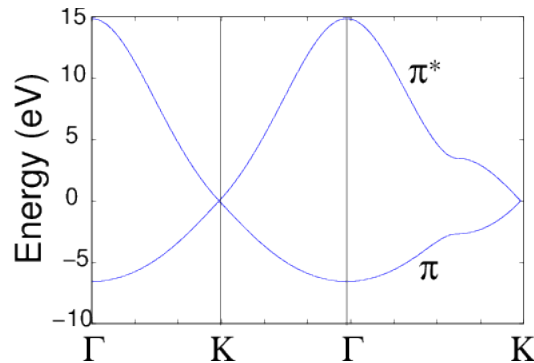
$$E^\mp(\vec{k}) = \mp t \sqrt{1 + 4 \cos\left(\frac{\sqrt{3}k_x a}{2}\right) \cos\left(\frac{k_y a}{2}\right) + \cos^2\left(\frac{k_y a}{2}\right)}\tag{3.36}$$

where t is the hopping matrix element between neighboring atoms. If we now plot the band structure between the special points in the Brillouin zone,

$$\begin{aligned}\Gamma \rightarrow M : \vec{k} = (k, 0) &\Rightarrow E^\mp(\vec{k}) = \mp t \sqrt{2 + 4 \cos\left(\frac{\sqrt{3}ka}{2}\right)} \\ M \rightarrow K : \vec{k} = \left(\frac{2\pi}{3a}, k\right) &\Rightarrow E^\mp(\vec{k}) = \mp t \sqrt{1 + 4 \cos\left(\frac{\pi}{\sqrt{3}}\right) \cos\left(\frac{ka}{2}\right) + \cos^2\left(\frac{ka}{2}\right)}\end{aligned}\tag{3.37}$$

$$K \rightarrow \Gamma : \vec{k} = (k, \sqrt{3}k) \Rightarrow E^\mp(\vec{k}) = \mp t \sqrt{1 + 5 \cos^2\left(\frac{\sqrt{3}ka}{2}\right)}\tag{3.38}$$

This band structure may be plotted as follows :



As seen in the figure, at the K points, the π and π^* bands touch at a single point. There are in fact 6 such equivalent points in the BZ of graphene. This is why ideal graphene is termed a *semimetal* or a *zero-gap semiconductor*. When graphene is rolled into a nanotube, there are two effects that determines the emergent band structure :

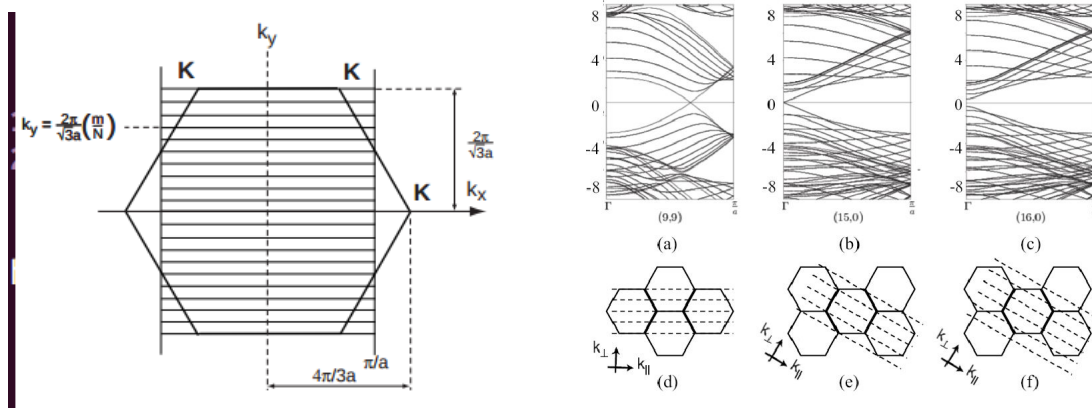


Figure 3.4: Allowed circumferential wavevectors (a) and band structures for nanotubes with different chiralities (b).

- The k -points along the circumference are quantized while remaining free in the perpendicular direction. This quantization results in the reduction of the available \vec{k} 's to be represented by lines in the BZ. Hence, whether a given nanotube is conducting or insulating is determined by whether these lines intersect any one of the K points.
- The previous item ignores the effect of curvature. Depending on how the nanotube is rolled, curvature may or may not open up a gap in what would otherwise be a conducting nanotube.

First, let us also ignore curvature. Although the nanotube may be rolled up along infinitely many different axis, we shall concentrate on the axis along $\vec{a}_1 + \vec{a}_2$, which corresponds to an (n, n) or *armchair* nanotube and along \vec{a}_1 (or equivalently $\vec{a}_1 - \vec{a}_2$), which in turn corresponds to an $(n, 0)$ or *zigzag* nanotube.

In the case of a zigzag nanotube with indices (n, n) , the circumference is an integer multiple of the norm of the sum of two lattice vectors, namely

$$C = \frac{4a}{\sqrt{3}}n. \quad (3.39)$$

The allowed wavevectors, which are in the k_x direction in accordance with the Cartesian axes fixed above, must then obey the rule

$$k_x C = k_x \frac{4a}{\sqrt{3}}n = 2\pi N \quad (3.40)$$

so as to accommodate an integral number of unbroken waves around the circumference. Eq. 3.40 then implies that the allowed wavevectors are given by $k_x = \frac{2\pi N \sqrt{3}}{4an}$. For $N = 0$, $k_x = 0$ and the line defined by this vector certainly passes through the K-points at the apex of the BZ. Thus, regardless of what n is all armchair nanotubes are (at least in the ideal case) metallic. The circumference of an $(n, 0)$ zig-zag nanotube is on the other hand

$$C = |\vec{a}_1 - \vec{a}_2| = |\vec{a}_1| = an \quad (3.41)$$

which yields the allowed vectors $k_y = \frac{2\pi N}{an}$. If we, for instance, concentrate on the K-point shown in the figure above, which has a y -coordinate of $\frac{4\pi}{3a}$ can accommodate $\frac{2n}{3}$ of the allowed k_y 's. When $n = 3m$ where $m = 1, 2, 3 \dots$, k_y will intersect with point K. Then we reach the conclusion that zigzag nanotubes are metallic only when n is an integer multiple of 3. In fact, one may generalize this rule to an (n, m) nanotube of arbitrary orientation. In that case the nanotube is metallic when $n - m$ is an integer multiple of 3.

4

Optical properties of confined structures

As the optical properties of structures gave to do which absorption and emission of electromagnetic ways, it is instructive to consider the interaction of such fields with matter at the nanoscale. The ingredients we need for this treatment are the Fermi's Golden rule (see the preliminary chapter)

$$w_{if} = \frac{2\pi}{\hbar} |H'_{if}|^2 \delta(E_f - E_i \mp \hbar\omega) \quad (4.1)$$

and the Hamiltonian in the presence of an electromagnetic field

$$H(\vec{r}, t) = \frac{1}{2m} \left[P + e\vec{A}(\vec{r}, t) \right]^2 - eV(\vec{r}, t) + U(\vec{r}). \quad (4.2)$$

In Eq. 4.2, $\vec{A}(\vec{r}, t)$ and $V(\vec{r}, t)$ are the vector and scalar potentials respectively. The magnetic field component of the electromagnetic field is given by the vector potential as

$$\vec{B} = \nabla \times \vec{A}. \quad (4.3)$$

Replacing the vector potential \vec{A} with $\vec{A} + \nabla\phi$ for an arbitrary ϕ does not change B , the choice of \vec{A} is arbitrary. Similarly, the electric field component given by

$$\vec{E}(\vec{r}, t) = -\nabla V(\vec{r}, t). \quad (4.4)$$

The results of the calculation, however, should not be affected by the choice of $\vec{A}(\vec{r}, t)$ and $V(\vec{r}, t)$. This is referred to as *gauge invariance*. A convenient choice is the Coulomb gauge which is given by

$$\nabla \cdot \vec{A} = 0 \quad \text{and} \quad V(\vec{r}, t) = 0. \quad (4.5)$$

With this gauge and noticing that

$$\left[P, \vec{A}(\vec{r}, t) \right] = -i\hbar \left[\nabla \cdot \vec{A}(\vec{r}, t) + \vec{A}(\vec{r}, t) \cdot \nabla \right] = 0, \quad (4.6)$$

the Hamiltonian in Eq. 4.2 simplifies to

$$H = \underbrace{\frac{P^2}{2m} + U(\vec{r})}_{H_0} + \underbrace{\frac{e}{m} \vec{A} \cdot P + \frac{e^2}{2m} \vec{A}^2}_{H'}. \quad (4.7)$$

In order to further simplify Eq. 4.7, we make the (quite justified) assumption that at the scales of the nanoparticles that we are interested in, the spatial variation of the vector field is imperceptible. In other words, the vector potential does not vary appreciably over the length scale of the

nanoparticle: $\vec{A}(\vec{r}, t) = A(t)\hat{e}$ where \hat{e} is the unit polarization vector. Due to the orthogonality of the solutions of H_0 , when the matrix element H'_{if} is calculated in Eq. 4.1, the term that is quadratic in \vec{A} yields zero. Finally, the perturbing Hamiltonian emerges as

$$H' = \frac{e}{m}\vec{A} \cdot P. \quad (4.8)$$

The corresponding matrix element in Fermi's Golden Rule is then

$$H'_{if} = \langle \Psi_i | H'(\vec{r}, t) | \Psi_f \rangle = \frac{e}{m} P_{if} A(t) \quad (4.9)$$

where $P_{if} = \langle \Psi_i | \hat{e} \cdot P | \Psi_f \rangle$ is the matrix element of the momentum operator. Finally, using the definition of the rate in Eq. 4.1,

$$w_{if} = \frac{2\pi}{\hbar} \left(\frac{e}{m_0} \right)^2 |P_{if}|^2 \delta(E_f - E_i \mp \hbar\omega). \quad (4.10)$$

Assuming a monochromatic perturbation of the form

$$A(t) = A_0 \cos(\omega t), \quad (4.11)$$

the time-averaged rate over one period is

$$\bar{w}_{if} = \frac{2\pi}{\hbar} \left(\frac{e}{m} \right)^2 |P_{if}|^2 \frac{A_0^2}{2} \delta(E_f - E_i \mp \hbar\omega). \quad (4.12)$$

\bar{w}_{if} , as described above is the rate of transition between a given initial state i and a given final state, f . Let us consider an two-dimensional infinite quantum well as an example. As described previously, the quantum well is free in the xy -plane, described by semi-continuous wave vectors, (k_x, k_y) and confined in the z direction, described by the quantum number n . The total transition rate out of state i and into any given state $f = (k_x, k_y, n)$ necessitates a sum over all possible final states:

$$\begin{aligned} \bar{W}_{if} &= \sum_n \sum_{k_x, k_y} \bar{w}_{if} \left[\underbrace{f(E_i)(1-f(E_f))}_{\text{absorption}} - \underbrace{f(E_f)(1-f(E_i))}_{\text{emission}} \right] \\ &= \sum_n \sum_{k_x, k_y} \bar{w}_{if} [f(E_i) - f(E_f)] \end{aligned} \quad (4.13)$$

In Eq. 4.13, two transition mechanisms are considered: *absorption* where a photon of frequency ω is absorbed to affect a transition from i to f where $E_f > E_i$ and *emission* where a photon is emitted while a transition occurs between states satisfying $E_f < E_i$. The function

$$f(E) = \frac{1}{e^{E/k_B T} + 1} \quad (4.14)$$

is the Fermi-Dirac distribution which gives the probability of a fermionic system to be in a state with energy E . The $f(E)$ terms seen in Eq. 4.13 ensures that there is exactly one electron in state i and none in state f in the case of absorption and the opposite in the case of emission. This is because states can have a fermionic occupation of at most one.

Through a simple comparison of decay of incident light into the material¹, the adsorption coefficient for a two-dimensional quantum well is given by

$$\alpha_{if} = \frac{2e^2}{\bar{n}\epsilon_0\omega m^2 c\pi L_z} \sum_n \int |P_{if}|^2 F_{if} \delta(E_f - E_i - \hbar\omega) d\vec{k}. \quad (4.15)$$

¹See, for example, p.358 of the third edition of *Quantum Wells, Wires and Dots* by Paul Harrison,

where \bar{n} , ε and c are the average index of refraction of the material, dielectric constant of vacuum and speed of light respectively. Finally, $F_{i,f} = f(E_i) - f(E_f)$. The details of the derivation of this equation is not central for the rest of this chapter and it is sufficient to understand that the total rate of transition out of the initial state i can be found by integrating² over all the available wave vectors of the final state as well as the index n that designates the discrete energy level of the quantum box in the z direction. Let us first deal with the dipole matrix element, $P_{i,f}$:

$$P_{i,f} = \frac{1}{A} \langle \psi_i(z) e^{i\vec{k}_i \cdot \vec{r}} | \hat{e} \cdot P | \psi_f(z) e^{i\vec{k}_f \cdot \vec{r}} \rangle dz d\vec{r} \quad (4.16)$$

where A is the lateral area of the sample (on the xy -plane), employed to fix normalization of the plane waves. The P_x and P_y components of the momentum operator give zero due to the orthonormality of the plane waves (as they are its eigenvectors). Hence, $P_{i,f}$ reads

$$P_{i,f} = \int_V \psi_f^*(z) P_z \psi_i(z) dz. \quad (4.17)$$

The area in the denominator disappears due to the integration on the xy -plane. Next, we utilize a well-known trick, which has to do with the commutation relation

$$\vec{P} = \frac{m}{i\hbar} [H_0, \vec{r}]. \quad (4.18)$$

Substituting Eq. 4.18 into Eq. 4.17 yields

$$\begin{aligned} P_{i,f} &= \frac{m}{i\hbar} \int \psi_f^*(z) (H_0 z - H_0 z) \psi_i(z) dz \\ &= -i \frac{m}{\hbar} (E_f - E_i) \int \psi_f^*(z) z \psi_i(z) dz = -im\omega d_{i,f} \end{aligned} \quad (4.19)$$

where the difference between the final and the initial energy is $\hbar\omega$, imposed by the Krönecker- δ in Eq. 4.15 and $d_{i,f}$ is the so-called dipole matrix element. In the case of the quantum well, $d_{i,f}$ can be calculated in a straightforward manner (let $n_f = n$ and $n_i = m$):

$$\begin{aligned} d_{i,f} &= \int z \sin\left(\frac{\pi z}{L_z} n\right) \sin\left(\frac{\pi z}{L_z} m\right) dz \\ &= \frac{1}{2} \int z \left[\cos\left(\frac{\pi z}{L_z} (n-m)\right) - \cos\left(\frac{\pi z}{L_z} (n+m)\right) \right] dz \end{aligned} \quad (4.20)$$

$$= \frac{L_z^2}{2\pi^2} \left[\frac{2}{(n-m)^2} - \frac{2}{(n+m)^2} \right] = \frac{L_z^2}{\pi^2} \frac{2nm}{(m^2 - n^2)^2}. \quad (4.21)$$

Substituting the result of Eq. 4.21 and Eq. 4.19 in Eq. 4.15 yields

$$\alpha_{i,f} = \frac{4e^2 L_z}{\bar{n}\varepsilon_0 m c \pi^2} \sum_n \frac{2nm}{(m^2 - n^2)^2} \int F_{i,f}(E_f, E_i) \delta(E_f - E_i - \hbar\omega) k dk \quad (4.22)$$

where the arguments of $f(E_f, E_i)$ have been made explicit for the sake of clarity and polar coordinates have been used in the integration variable taking advantage of the directionally symmetric form of the energy in $\vec{k} = (k_x, k_y)$. Here let us remember that $E_f = \frac{\hbar^2 k^2}{2m} + E_n$. Affecting a change of variables such Noticing that

$$dE_f = \frac{\hbar^2}{m} k dk \quad (4.23)$$

²The original sum was converted into an integral for the sake of convenience using the method introduced during the calculation of density of states

Eq. 4.22 becomes

$$\begin{aligned}
\alpha_{if} &= \frac{16e^2 L_z}{\bar{n}\varepsilon_0 c \hbar^2} \sum_n \frac{2nm}{(m^2 - n^2)^2} \int F_{if}(E_f, E_i) \delta(E_f - E_i - \hbar\omega) dE_f \\
&= \frac{16e^2 L_z}{\bar{n}\varepsilon_0 c \hbar^2} F_{if}(E_i + \hbar\omega, E_i) \sum_n \frac{2nm}{(m^2 - n^2)^2}
\end{aligned} \tag{4.24}$$